8th AIAA/CEAS Aeroacoustics Conference & Exhibit
 <font color="green">Fire
17-19 June 2002, Breckenridge, Colorado

AIAA 2002-2427

FAN NOISE SOURCE DIAGNOSTIC TEST—FAR-FIELD ACOUSTIC RESULTS

Richard P. Woodward,* Christopher E. Hughes,*
Robert J. Jeracki, and Christopher J. Miller*
National Aeronautics and Space Administration
Glenn Research Center
Cleveland, Ohio 44135

Abstract

A comprehensive model fan source diagnostic test was conducted in the NASA Glenn Research Center 9x15 Low Speed Wind Tunnel. Far field acoustic data were acquired at 0.10M, which is representative of aircraft approach/takeoff conditions. Concurrent data (reported elsewhere) were taken to quantify the radiating modal field, rotor wake characteristics (laser-Doppler velocimeter), and detailed aerodynamic performance measurements, thus giving a comprehensive view of the fan noise-generation mechanisms. This report presents an overview of the far-field acoustic results for this fan test. The research fan hardware consisted of two rotors and three stator sets. Far-field acoustic results are presented which show the effect of rotor blade loading and wake distribution, stator vane number (cuton and cutoff for the rotor BPF tone) and stator sweep. The cuton swept stator was typically the quietest stator configuration. A Rotor-Alone Nacelle (RAN) configuration (with no downstream stator) was also tested in which the nacelle was externally supported and actively centered on the rotor. Acoustic results showed that designing for a higher rotor speed but with reduced blade unit area loading may significantly reduce overall fan stage noise, especially at subsonic rotor tip speeds. The RAN results showed that stator-induced noise might account for 4 or more EPNdB at lower fan speeds. Acoustic results are presented in terms of flyover effective perceived noise and sound power level. An analysis code was used to show the acoustic effect of selectively removing the fundamental BPF tone and all harmonics thereof. Significant noise benefits may be realized with active noise control and/or tuned duct liners to reduce the fundamental BPF tone near the rotor transonic condition.

Introduction

A major source of aircraft engine noise comes from the interaction of the rotor viscous wake with the exit guide vanes, or stators. The most prominent components of this interaction noise are tones at multiples of the rotor blade passage frequency, although there also exists a broadband component of this rotor-stator noise. Traditional methods of reducing this interaction noise have been to select blade/vane ratios to satisfy the cutoff criterion for propagation of the fundamental rotor tone[1] and increased axial spacing between the rotor and stator.[2] Stator sweep or stator sweep and lean have been shown to significantly reduce BPF tone noise with some additional noise reduction often seen for the broadband noise as well.[3–6]

The Source Diagnostic Test (SDT) was conduced in the NASA Glenn Research Center 9x15 Low Speed Anechoic Wind Tunnel (LSWT) as a comprehensive investigation of fan stage noise generation mechanisms. This report presents an overview of the far-field acoustic results from that test series. The test fan was a 1/5th scale model of a modern high bypass ratio turbofan. It was designed by General Electric Aircraft Engines (GEAE) under an internal research and development program and was provided to NASA as part of a cooperative research effort for this test. This test series investigated the effect of changes in rotor design tip speed, unit area blade loading, rotor tip clearance, stator configuration (cutoff and cuton radial vanes with respect to the BPF tone, and cuton swept vanes), and a unique rotor-alone configuration with no stator or downstream internal support struts. This Rotor-Alone Nacelle (RAN) test allowed an investigation of rotor noise generation without the presence of stator noise, thus revealing potential noise benefits obtainable from a fan stage without stator interaction noise.

The SDT series was designed to give a comprehensive understanding of turbofan noise generation mechanisms. Concurrent comprehensive aerodynamic measurements were made for the R4 rotor test configurations,[7–8] as well as internal laser Doppler velocimeter[9–10] and rotating microphone modal measurements.[11] This paper will present an overview of the far field acoustic results from this test series.

*Member, AIAA.

Description of Fan Test

Research Fan

Figure 1 is a photograph of the model fan installed in the NASA Glenn 9x15 LSWT. Acoustic data were taken with a free stream Mach number of 0.10 which is sufficient to achieve acoustic flight effect[12] and provides far-field acoustic data representative of takeoff/approach operation. All data were taken at 0° fan axis angle of attack. The fan stage did not have a simulated core flow.

The NASA Glenn Ultra High Bypass (UHB) drive rig[13] was used to power the SDT model fan. The UHB rig was powered by a high-pressure air turbine drive with the drive air and instrumentation supplied through the floor-mounted support strut, as shown in figure 1. The drive turbine exhaust air was ducted downstream through an acoustically treated diffuser and exited the end of the treated test section. There was little indication of acoustic contamination of the aft fan data from the turbine exhaust.

Acoustic data were also taken with a rotor-alone configuration with no internal downstream support struts or stators. This RAN configuration was a continuation of an earlier rotor-alone fan tests to isolate the relative rotor and stator contributions to fan broadband noise.[14] References 15 and 16 present results for a model rotor which could be run with/without outlet guide vanes to isolate rotor-alone noise in a fan stage.

The RAN nacelle was supported by a twin strut assembly (Fig. 2) mounted on a precise positioning table fastened to the tunnel wall. Rotor tip clearance was maintained through a four laser positioning system that tracked small transverse movements of the rotor and adjusted the nacelle position accordingly.

The primary test rotor, designated R4 (Fig. 3), was representative of an early GE90 engine fan. A second rotor, designated M5, was designed for a 10% higher tip speed with a slightly higher stage pressure ratio (Table I). Both rotors had 22 blades, resulting in a somewhat lower loading per blade for the M5 rotor. Also shown in figure 3 is a sketch of the rotor-alone nacelle (RAN) installation.

The fan stage was tested with three sets of outlet guide vanes, or stators. These were designed for similar aerodynamic performance (Table I). The 54-vane baseline radial stator (Fig. 4) was cutoff for propagation of the fundamental BPF tone. The radial "low-count" stator (Fig. 5) was cuton with 26 vanes as was the 26-vane swept "low-noise" stator (Fig. 6). The vane aspect ratios of all three stator sets were adjusted to maintain the same solidity. Reductions in stator vane count have been shown to reduce broadband noise levels.[15] The swept stator had 30° of sweep, an amount of sweep that has been shown to significantly reduce BPF tone levels in prior fan tests.

Anechoic Wind Tunnel and Acoustic Instrumentation

The NASA Glenn 9x15 LSWT is located in the low speed return leg of the 8x6 Supersonic Wind Tunnel. The tunnel test section walls, floor, and ceiling have acoustic treatment to produce an anechoic test environment.[17–19] Figure 7 is a sketch of the test fan installed in the 9x15 LSWT. Sideline acoustic data were acquired with a computer-controlled translating microphone probe (also seen in the photograph of Fig. 1) and with three aft microphone assemblies mounted to the tunnel floor. The translating microphone probe acquired data at 48 sideline geometric angles from 27.2 to 134.6° relative to the fan rotor plane. The translating probe traverse was 227 cm (89 in.) from the fan rotational axis (about four fan diameters). A wall-mounted microphone probe was placed at a reference location adjacent to the translating probe home position (134.6°, maximum aft travel). The three fixed microphone assemblies were mounted at the home axial position to acquire aft acoustic data at geometric angles of 140, 150, and 160°. Data were also acquired with an acoustic barrier wall installed adjacent to the fan which effectively blocked aft-radiated fan noise (Fig. 8). The acoustic data were acquired through a digital computer system and stored for post-run analysis.

Results and Discussion

Aerodynamic Performance

Figure 9 shows representative aerodynamic performance for the R4 and M5 fans with the 54-vane baseline stator.[7] The two rotors operated on essentially the same operating line (Fig. 9(a)). The M5 rotor was designed for a 10% higher tip speed and a corresponding lower blade loading per unit area relative to the R4 rotor. The two rotors showed essentially the same fan pressure ratio and corrected inlet weight flow at 50% design fan speed. However, the M5 rotor achieved an increasingly higher PR and weight flow than the R4 rotor with increasing percent fan speed.

Acoustic comparisons between the R4 and M5 rotor configurations are based on percent design fan speed. Percent fan speed gives a first-order approximation of fan stage thrust, although the fan stage thrust (analogous to stage pressure ratio) was somewhat higher for the M5 rotor with increasing percent design fan speed. Modest differences in fan stage thrust should not have a significant impact on comparing acoustic

results. Fan noise has been shown to follow the relationship 10log ($thrust_1/thrust_2$). Assuming that thrust differences follow stage pressure rise differences, the worst-case acoustic error near fan design speed would be 10log (0.50/0.47) = 0.27 dB. Thus acoustic comparisons based on similar "percent design speed" for R4 and M5 should be valid.

Figure 9(b) shows the fan pressure ratio as a function of corrected rotor tip speed. The 10% higher design speed of the M5 rotor is clearly evident in the R4 and M5 data.

Acoustic Performance

Acoustic Data Reduction

All of the fan acoustic data were acquired at 0.10 tunnel mach. Sideline data are presented in terms of emission angles. The emission angles are related to the geometric, or observed angles by the relationship:

$$\Theta_{em} = \Theta_{geom} - \sin^{-1} (M_0 \sin \Theta_{geom})$$

where Θ_{em} and Θ_{geom} are, respectively, the emission and observed sideline angles, and M_0 is the test section mach number. The observed angles for the sideline translating microphone probe are then 25° to 130°, and the three fixed microphones measure aft observed angles of 136, 147, and 158°. This angular range was sufficient to define the sideline noise profile for this aft-dominated fan for subsequent EPNL calculations.

Digital acoustic data were processed as constant bandwidth spectra. Spectra were acquired and averaged at each translating probe or fixed mic position with 6 and 59 Hz bandwidths. These constant bandwidth spectra were electronically merged and used to generate 1/3-octave spectra. An acoustic analysis code was used to generate sound power level spectra (PWL). This code had provisions for specifying the frequency and sideline angular ranges of interest.

A flyover effective perceived noise level code was used to generate relative flyover EPNL values at a 457 m (1500 ft.) altitude. The code could selectively remove spectral tones to show relative EPNL changes associated with removal of bypass and core tones. Results from this analysis code show relative EPNdB values for various configurations, and are not intended to be representative of any particular aircraft.

Baseline 54-Vane Radial Stator

Figure 10 shows EPNL for the cutoff baseline stator with all spectral tones present. Noise levels are plotted against percent of design fan speed, which allows for a comparison of the R4 and the higher-speed M5 rotors. The rotor-alone nacelle (RAN) results give an indication of the possible noise "floor" attainable without any stator interaction noise. However, RAN results are currently only available for R4 rotor. It is likely that RAN acoustic results for the M5 rotor may be somewhat different.

Total flyover results (Fig. 10(a)) shows that the M5 rotor is about 3 EPNdB higher noise level than the R4 rotor near the designated cutback fan speed. The M5 rotor is slightly quieter (about 1 EPNdB) at lower fan speeds, and about the same as the R4 rotor near design fan speed. These noise differences are more significant for inlet-radiated noise with the acoustic barrier wall in place (Fig. 10(b)). Inlet-radiated EPNL for the M5 rotor peaks at over 9 EPNdB higher than for the R4 rotor at just below cutback fan speed. However, inlet-radiated noise levels for the M5 rotor are 1 to 3 EPNdB lower than for the R4 rotor at subsonic fan speed, and about 1 EPNdB lower near design fan speed.

The RAN results in figure 10 give an indication of stator-induced noise. The R4 rotor without a stator present is about 4.5 EPNdB quieter at subsonic fan speeds than the noise level for that rotor with the baseline stator present. It is only near design speed that noise levels for the R4 RAN configuration approach those of the baseline stator. The RAN configuration was only tested for the R4 rotor. Noise levels for a RAN configuration with the M5 rotor would likely show a similar noise decrease relative to the baseline stator configuration.

Testing with the RAN configuration posed a unique a unique acoustic (and aerodynamic) problem. The fan exit guide vanes or stators effectively removed swirl from the exhaust airflow; however exhaust flow for the RAN configuration still retained significant swirl. Additionally, the diameter of the drive rig housing decreased downstream of the fan exit nozzle (see Fig. 8). Consequently, the conservation of flow angular momentum resulted in an even more severe swirl as the exit flow approached the drive support pylon. This exit flow problem resulted in excessive downstream noise levels for the initial RAN tests. This flow problem was largely alleviated with a constant diameter downstream fairing for the drive rig and an angled leading edge attachment for the drive rig pylon that helped to guide the angular airflow onto the axial support pylon airfoil.

The M5 rotor (designed for a higher tip speed) becomes transonic at a lower percent design fan speed than does the R4 rotor. This earlier onset of rotor-alone tone and possibly multiple pure tones causes a sharp increase in the M5 noise levels at about 80% design

speed (which is below designated cutback speed for that fan), whereas the corresponding noise level increase for the R4 rotor occurs just above 87.5% speed (designated cutback speed for the R4 fan).

An analysis code was used to remove the tone (BPF) from the EPNL calculations. Removal of this tone (Fig. 11) significantly reduces the higher M5 noise levels near cutback. The overall flyover EPNL with the BPF tone removed (Fig. 11(a)) results in the M5 rotor being less than 1 EPNdB noisier than the R4 rotor near designated cutback speed.

As might be expected, acoustic results for the R4 RAN configuration showed little BPF and harmonic tone content at subsonic fan speeds. Consequently, the RAN results in figure 11 only show a reduction with tone removal at higher, transonic fan speeds and above where rotor-alone tones become cuton.

Removal of the BPF tone was also beneficial for the forward-radiated noise (Fig. 11(b)), although the M5 noise levels are still about 4 EPNdB higher than the R4 levels near cutback, indicating a significantly higher tone harmonic content in the M5 spectra. Removal of this tone was especially beneficial for the R4 rotor at 90% fan speed, where the rotor-alone tone became significant.

Figure 12 shows the EPNL with all harmonics (nBPF) of the fundamental tone removed. Removal of these tones significantly reduced the overall EPNL (Fig. 12(a)) for both rotors in the 80 through 95% design speed range. Removal of the nBPF tones (Fig. 12(b)) gave additional benefit for the M5 rotor at 85% design fan speed.

Sound power level (PWL) spectra give a comprehensive overall view of the acoustic spectra. PWL spectra are shown at designated approach speed (nominal 61% design), cutback (nominal 86% design) and 100% design speed, respectively, in figures 13 through 15, for 6 and 59Hz bandwidth spectra with/without the acoustic barrier wall in place. The 6 Hz bandwidth spectra are considered valid only through 7 KHz due to data "roll off."

The PWL spectra at approach fan speed (Fig. 13) show a significant noise reduction associated with the M5 rotor at frequencies below 7 KHz. As expected, the fundamental BPF tone is essentially cutoff, but the 2BPF tone is present in the spectra. The RAN configuration PWL results show that removal of the stator reduced the broadband noise by up to 5 dB.

Multiple pure tones and rotor-alone BPF tone are significant for the M5 rotor at the nominal cutback fan speed (Fig. 14). The R4 rotor-alone BPF tone is evident, although lower, at this fan speed. However, MPTs have not yet evolved for the R4 rotor. Broadband noise levels for the M5 rotor (as interpreted between MPT spikes) are about 2 dB lower than for the R4 rotor. RAN results at this fan speed showed a more modest reduction in broadband noise above 4 KHz, but a noise increase at lower frequencies. This low-frequency RAN noise is more significant without the barrier wall present, showing that it most likely comes from the previously discussed exit flow swirl noise problem associated with the RAN configuration.

There are significant differences between the PWL spectra for the two rotors at design fan speed (Fig. 15). The fundamental BPF tone level is about the same for the two rotors with the baseline stator and without the acoustic barrier wall. The BPF tone level for R4 in the RAN configuration is about 7 dB lower, indicating that BPF tone noise, which tends to be aft-dominate at higher fan speeds, is significant at design fan speed in the total flyover spectra. The R4 rotor-alone results show a somewhat lower BPF tone level, consistent with the absence of a BPF tone contribution. The R4 BPF tone levels are identical with/without the baseline stator and with the acoustic barrier wall in place, thus suggesting that the inlet-radiated tone noise for the R4 rotor is essentially rotor-alone. Also, the broadband noise level for the M5 rotor is now about 3 dB higher than the R4 broadband level at frequencies below 4 KHz.

RAN noise levels at design speed show a significant broadband increase at lower frequencies, thought to be associated with exit flow swirl for the RAN configuration. R4 BPF tone levels are essentially the same for the RAN and baseline stator configurations with the barrier wall present. In the absence of the barrier wall the R4 BPF is somewhat higher with the stator present. This result shows that tone noise originating from stator interaction at design fan speed is highly aft radiating while inlet-radiating tone noise arising form the cuton rotor-alone field is not affected by the presence of the stator.

26-Vane Radial Stator

The 26-vane radial stator is cuton with respect to the fundamental BPF tone; however, the lower number of stator vanes is expected to somewhat lower the broadband noise of the spectra. Figures 16 to 21 show acoustic results for this stator corresponding to what was shown for the baseline stator in figures 10 to 15.

The EPNL for the M5 rotor is significantly lower than that for the R4 rotor at subsonic fan speeds with all interaction tones present (Fig. 16). Figure 16(a) shows EPNL for the overall flyover. Noise levels for the M5 rotor are about 2 EPNdB lower than those for the reference R4/baseline stator at fan speeds up to approach, while the R4 noise levels with this stator are about 3 EPNdB higher than the baseline reference. Noise levels for both rotors are about the same above

75% design speed, both showing about 2-1/2 EPNB above baseline near cutback. Inlet-radiated noise for the M5 rotor (Fig. 16(b)) is similar to what was shown with the baseline stator in figure 10(b) with a significant noise peak near cutback.

Podboy, et al. present flow field measurements made downstream of these two rotors operating at approach and takeoff fan speeds. These Laser Doppler velocimeter (LDV) measurements indicate that the two fans generate significantly different wake flows, especially at the approach operating condition. The main difference is in the lean of the blade wakes over the outer 20% of span. The outer portions of the M5 blade wakes lean in the direction opposite of the rotor rotation, while the R4 wakes are much more radial. As explained in reference 10, this difference is expected to account for significant differences in the BPF tone noise generated by these two fan stages at the approach operating condition. This is confirmed by the acoustic results presented herein.

Removal of the Blade Passage Frequency (BPF) tone with this stator would be expected to show the benefits of reduced vane number without the acoustic penalty of being "cuton." Figure 17 shows the EPNL with the fundamental BPF tone removed for the 26-vane radial stator. Removal of this tone for the overall flyover (Fig. 17(a)) was especially beneficial for the R4 rotor, bringing that level essentially to that of the reference R4/baseline stator with all tones present. Noise levels for the M5 rotor with the BPF tone removed are at or below those for the R4 rotor throughout the fan speed range. Removal of the BPF tone with the barrier wall in place (Fig. 17(b)) made little change in the R4 EPNL except at 90% fan speed where removal of the fundamental rotor-alone tone reduced the EPNL by about 5 dB. The M5 noise peak just above cutback speed was reduced by about 4 EPNdB by removal of the fundamental tone.

There is still a significant acoustic benefit associated with removal of all harmonics of the BPF tone (Fig. 18). Removal of these tones reduced the R4 tone levels by almost 2 EPNdB relative to the reference R4/baseline stator throughout the fan speed range (Fig. 18(a)). Noise levels for the M5 rotor were about 3 EPNdB below baseline through cutback fan speed. Inlet-radiating noise levels for the R4 rotor (Fig. 18(b)) were likewise reduced with removal of all harmonics of the fundamental tone.

As expected, the rotor interaction tone levels in the PWL spectra at approach fan speed are much higher for the R4 rotor in the region of approach fan speed (Fig. 19). Broadband noise levels for the M5 rotor were about 2 dB below R4 rotor levels at lower frequencies, as was seen earlier for the baseline stator. The PWL spectra at cutback fan speed (Fig. 20) were similar to what was seen at this speed for the baseline stator, with the M5 rotor showing the higher interaction tone levels. At 100% design fan speed (Fig. 21) the overall BPF tone levels for the two rotors with the 26-vane radial stator are about the same, with the R4/RAN tone being slightly lower. However, with the barrier wall in place, the inlet-radiating BPF tone for the R4 rotor is higher than that for the M5 rotor, suggesting that rotor-alone noise for the M5 rotor is less than that for the R4 rotor at design fan speed.

26-Vane Swept Stator

Stator sweep (and lean) has been shown to significantly reduce rotor-stator interaction tone levels as well as somewhat reduce broadband noise levels. Thus, the 26-vane swept stator had the potential to demonstrate the benefits of stator sweep (hopefully negating the acoustic penalty of being cuton) while also retaining the acoustic benefit associated with reduced vane number relative to the baseline (54-vane) stator.

Stator sweep was highly beneficial for the R4 rotor. As shown in figure 22(a) for the overall flyover EPNL, noise levels for the R4 rotor and the swept stator were essentially the same as for the baseline stator (and significantly below those for the 26-vane radial stator) up to cutback fan speed, and then about 1-1/2 EPNdB below baseline at higher fan speeds. Noise levels were also reduced at lower fan speeds for the M5 rotor. Likewise, inlet-radiated noise levels (Fig. 22(b)) for the R4 rotor/swept stator were at or below the reference baseline. Inlet radiated noise for the M5 rotor/swept stator was only slightly reduced from that with the 26-vane radial stator, and continued to show high levels at 90% fan speed.

Stator sweep was not entirely effective in removing rotor-stator interaction tones for this cuton stator. As shown in figure 23(a), removal of the BPF tone resulted in an additional reduction in overall flyover noise for the two rotors. However, removal of this tone had little additional benefit on the inlet-radiated noise at fan speeds away from cutback (Fig. 23(b)) Removal of the BPF tone resulted in a 5 EPNdB reduction for the R4 rotor at 90% speed, and a significant reduction in noise for the M5 rotor at 86% speed. Removal of all harmonics of the BPF tone (Fig. 24) was effective near the cutback fan speed for both rotors.

Figure 25 shows PWL spectra at the nominal approach fan speed. There were still strong rotor-stator interaction tones for the R4 rotor/swept stator, while these tones are hardly seen for the M5 rotor. The broadband levels for the M5 rotor continue to be lower than for the R4 rotor at frequencies below 5 KHz. At higher frequencies the R4 and M5 broadband levels are the same with the barrier wall present, but higher for

the M5 rotor with the wall removed; suggesting that the higher M5 broadband levels with the swept stator are essentially aft radiating.

At cutback fan speed (Fig. 26) the M5 rotor-alone BPF tone is well established, and higher than that for the R4 rotor. The M5 rotor continues to show slightly lower broadband levels at low frequencies. PWL spectra results at design fan speed for the swept stator (Fig. 27) are similar to what was seen for the 26-vane radial stator, with the R4 rotor now showing lower broadband levels.

Comparison of Three Stator Sets

Figure 28 shows sound power levels for the first two tone orders (BPF and 2BPF) as a function of rotor physical tangential tip speed taken from the overall, 59 Hz bandwidth PWL spectra. Results for the R4 rotor (Fig. 28(a)) show that the BPF tone is lowest for the baseline cutoff stator, and highest for the 26-vane radial stator up to transonic fan speed, where the rotor-alone BPF tone dominates the spectra. The 2BPF tone is nearly the same for the baseline and 26-vane swept stators (except at supersonic fan speeds where the baseline is slightly noisier), and somewhat higher for the 26-vane radial stator.

Tone levels for the R4 RAN configuration were significantly lower than those with the stators present. The RAN tone could not be detected in many of the subsonic rotor speed spectra; hence the broadband level at the expected tone frequency was used to represent the tone. As previously mentioned, tone levels for the RAN configuration tended to merge with those for the stator configurations at higher fan speeds where the rotor noise field was cuton.

The BPF tone tended to be lower for the M5 rotor at subsonic fan speeds. The BPF tone results for this rotor (Fig. 28(b)) showed the same trends as for the R4 rotor, but at lower overall noise levels. The 2BPF tone level for the M5 rotor was typically up to 5 dB lower for the swept stator than for the baseline and 26-vane radial stators; 2BPF results for the two radial stators were essential the same.

Figure 29 shows the tone PWL with the acoustic barrier wall in place. The trends are similar for the R4 rotor, although the difference in noise levels is less than was observed for the overall spectra. The inlet-radiated BPF tone level (Fig. 29(b)) for the M5 rotor shows little change with stator configuration except at the lowest fan speeds where the 26-vane radial stator is somewhat noisier. This is consistent with the rotor wake results of reference 10, which predicted that the reduced wake of the M5 rotor would result in less rotor-stator interaction noise. The forward-radiating 2BPF tone noise for the M5 rotor is lowest for the baseline stator at subsonic fan speeds.

The comparison of acoustic performance for the three stator sets and two rotors has shown that the overall perceived noise levels can be lower for a particular rotor/stator combination even though the respective interaction tone levels may not follow the same trend. That is, while tone noise is an important component of the overall noise, a significant reduction in associated broadband noise level may actually control the EPNL. Figure 30 shows the overall sound power level (OAPWL, integrated from 1 K to 50 KHz) for the three stators and two rotors, and the RAN configuration as a function of fan tip speed. OAPWL for the RAN configuration without the barrier wall present (Fig. 30(a)) was about 5 dB lower than any of the stator configurations at subsonic fan speeds. Otherwise, the swept stator showed the lowest OAPWL with each rotor.

RAN noise levels with the barrier wall present (forward-radiating noise) were lower than for the stator configurations, but not to the degree that was shown for the no wall data. Removal of the stator, of course, essentially removed the interaction tones at subsonic fan speeds. However, a significant broadband noise reduction was also seen with the stator removed. The fact that the RAN noise reduction was greatest with no barrier wall shows that much of this broadband noise is aft radiating.

It is possible to obtain an approximation of the aft-radiating sound power by subtracting the forward-radiating PWL (with barrier wall) from the total sideline PWL. Figures 31 to 33 show total, forward-radiating, and aft-radiating sound power levels for the R4 rotor with the 0.020 in. tip clearance. The results for the BPF and 2BPF tones are typically approximated as the corresponding broadband levels at tone frequencies for the RAN BPF and 2BPF tones, and for the cutoff baseline stator BPF tone at subsonic tip speeds.

The PWL split for the BPF tone is shown in figure 31. Again, the RAN configuration had essentially no BPF and 2BPF tones at subsonic rotor tip speeds, with rotor-locked tones becoming significant at transonic and higher speeds. These results show that the RAN BPF tone is forward dominated at the higher, rotor-locked fan speeds. This is also typically the case for the three stator configurations near the transonic fan speed; however, the forward-radiated tone levels for the stator configurations tend to fall off at the highest fan speeds. Rotor-stator interaction BPF tends to be aft dominant when cuton at subsonic fan speeds, as shown for the 26-vane radial and swept stators.

The 2BPF tone is cuton for all stator configurations (Fig. 32). The RAN results show essentially equal

forward and aft levels except at the transonic condition where the inlet-radiated noise is dominated by the direct rotor field. The dip in the estimated aft-radiated noise level at transonic speed is probably due to calculation (decibel subtraction) errors due to the essentially same measured inlet and total tone levels. The 2BPF tone for the baseline stator is strongly aft dominated throughout range of fan speeds. Interestingly, the forward radiated 2BPF tone for the 26 vane stators through subsonic fan speeds is less aft dominated than was the BPF tone.

The overall sound power level (integrated 1 to 50 KHz, Fig. 33) is inclusive of both tone and broadband noise. RAN OAPWL for forward and estimated aft radiation is essentially the same at lower fan speeds, however the OAPWL becomes more aft dominated above 900 ft./s tip speed. OAPWL for the three stator configurations is likewise aft dominated throughout the fan speed range although the inlet radiated noise becomes significant at and slightly above transonic fan speed.

Effect of Rotor Tip Clearance

The R4 rotor was tested with three rotor tip clearances with the three research stator sets. The "nominal" tip clearance was achieved with a "rub in" of the outer flow path rub strip at maximum fan speed. Additional tip clearances were 0.020 in. (used in the data comparisons presented herein as representative of a "worn" engine), and 0.030 in. The 0.020 in. and 0.030 in. tip clearances were estimated for the fan at design speed. Recent revisions of the likely rotor tip clearances at design speed have suggested that the designated 0.020 in. and 0.030 in. tip clearances may, in fact be slightly tighter. However, the designated values will be used for consistency with other concurrent reports on the SDT results.

Figure 34 shows the delta EPNL relative to the 0.020 in. tip clearance for the three stator sets. The greatest effect of tip clearance was seen with the cuton 26-vane radial stator, with a noise spread of almost 1 EPNdB. The cutoff baseline stator showed the least sensitivity to rotor tip clearance. The M5 rotor was only tested with one tip clearance, hence similar comparisons are not available for that rotor.

The effect of rotor tip clearance on the BPF and 2BPF tone levels is shown in figure 35. These tone levels were taken from the 59 Hz bandwidth PWL spectra. As might be expected, the BPF tone level is typically highest with the 0.030 in. tip clearance and lowest with the nominal tip clearance, although there are significant level changes relative to the 0.020 in. baseline with fan speed. Results for the 2BPF tone are less reasonable, with the nominal tip clearance showing the highest level for the baseline and 26-vane swept stators. The BPF results for the 26-vane radial stator (which typically showed the highest stator interaction tone levels) follows the expected trend of increasing noise with increasing rotor tip clearance.

Concluding Remarks

The research fan hardware consisted of two rotors and three stator sets. The reference rotor, designated R4, was designed for a 1215 ft./s tip speed, while the second rotor, designated M5, was designed for a 10% higher tip speed (1350 ft./s). The overall fan stage pressure ratio was similar with both rotors (1.47 versus 1.50), however, the higher tip speed of the M5 rotor resulted in a lower loading/unit blade area. The fan stage was tested with three research stators, each designed to give equivalent aerodynamic performance. The baseline 54-vane baseline radial stator was cutoff with respect to propagation of the fundamental BPF tone. The 26-vane radial and 26-vane swept stators were cuton. Acoustic data were also taken for the R4 rotor without a downstream stator, revealing the noise contribution of the stator vane sets. Far-field acoustic data were taken with/without an acoustic barrier wall, showing the overall and inlet-radiating noise field. Aft-radiating noise could be approximated by subtraction of the inlet noise from the overall noise levels.

The M5 rotor typically showed lower noise levels than did the R4 rotor at subsonic fan speeds. This noise reduction is consistent with LDV measurements that showed the M5 rotor wake to be less severe than that for the R4 rotor at similar operating conditions. However, the M5 rotor was often noisier at the higher, transonic and above, fan speeds where the rotor-alone noise is cuton.

- Noise levels were significantly higher for the R4 rotor and the 26-vane radial stator than for the M5 rotor and that stator at subsonic fan speeds.
- As expected, the lowest noise levels were typically associated with the swept stator. This stator had the benefit of stator sweep; but, unlike the baseline stator, was cuton. Thus, there were conflicting effects of noise reduction through stator sweep and reduced vane number but being cuton. The benefits of cuton swept stators exceed the penalty of the cuton BPF tone.
- An acoustic analysis code was used to selectively remove the fundamental (BPF) and harmonic (nBPF) tones for the flyover EPNL calculations. Removal of the BPF tone (possible through active noise control or tuned duct liners) showed that there was no significant EPNL noise reduction associated with reducing the radial stator vane count, but did show a

2 EPNdB reduction with stator sweep at lower fan speeds. Removal of all tones (nBPF) gave a 3 EPNdB reduction for the swept stator and a more modest 1 EPNdB reduction for the 26-vane radial stator relative to the 54-vane baseline stator.

- The R4 rotor was run in a Rotor Alone Nacelle (RAN) configuration without a downstream stator. Fan exit flow swirl resulted in significant broadband noise at higher fan speeds and lower frequencies. The severity of this problem was somewhat relieved by the addition of a cylindrical fairing to the downstream fan housing and the addition of an angled transition airfoil to the drive support pylon.
- The RAN data enabled a separation of rotor and stator induced noise. Stator induced noise was shown to have significant broadband as well as tone noise components; however, at transonic and higher rotor speeds the cuton rotor noise field dominated the noise. Removal of the stators reduced EPNL at subsonic rotor speeds by as much as 4.5 dB.
- RAN results at design fan speed showed that the cuton rotor noise field (at transonic and above fan speeds) rather than stator interaction dominated forward-radiating tone noise while aft-radiating noise had a significant stator interaction component.
- Rotor-locked BPF and 2BPF tone PWL levels for the RAN configuration were forward dominated at transonic fan speed; OAPWL, which included broadband contributions, showed the rotor-alone to be more strongly aft dominated at higher subsonic fan speeds.
- Cuton BPF and 2BPF tone PWL for the stator configurations were strongly aft dominated, although forward-radiating tone PWL became significant near the transonic fan speed region.
- Data were also taken to evaluate the acoustic effect of rotor tip clearance for the R4 rotor. Noise levels generally showed a small increase with increasing tip clearance with these effects being most noticeable with the R4 rotor and 26-vane radial stator.

Acknowledgements

Acknowledgement is given to General Electric Aircraft Engines for designing the R4 and M5 model fans and providing it to NASA as the current technology bypass fan baseline for this test. Also, GEAE designed and fabricated the three model OGV configurations and model nacelle used in this test under NASA Contract NAS3-26617, Task Order 63 and NAS3-98004, Task Order 7. Mr. Philip Gliebe (GEAE) who led the initial fan Source Diagnostic Test as part of the AST Noise Reduction Program, provided valuable insight on fan noise sources.

Acknowledgement is also given to the Boeing Aircraft for their earlier tests of a model fan with/without the presence of a downstream stator. These Boeing results provided the insight for the current effort to obtain far-field acoustic results for a rotor-alone nacelle configuration.

References

1. Tyler, J.M. and Sofrin, T.G., "Axial Flow Compressor Noise Studies," SAE Trans., Vol. 70, 1962, pp. 309–332.
2. Woodward, R.P., and Glaser, F.W., "Wind Tunnel Measurements of Blade/Vane Ratio and Spacing Effects on Fan Noise," AIAA Journal of Aircraft, Vol. 20, No. 1, January 1983, pp. 58–65.
3. Kazin, S.B., "Radially Leaned Outlet Guide Vanes for Fan Source Noise Reduction," NASA CR–134486, November. 1973.
4. Envia, E., Huff, D.L., and Morrison, C.R., "Analytical Assessment of Stator Sweep and Lean in Reducing Rotor-Stator Tone Noise," AIAA–96–1791, May 1996.
5. Woodward, R.P., Elliott, D.M., Hughes, C.E., and Berton, J.J., "Benefits of Swept and Leaned Stators for Fan Noise Reduction," AIAA–99–0479, January 1998, Journal of Aircraft, vol. 38, no. 6, November-December, 2002, pp. 1130–1138.
6. Woodward, R.P., Gazzaniga, J.A., Bartos, L.J., and Hughes, C.E., "Acoustic Benefits of Stator Sweep and Lean for a High Tip Speed Fan," AIAA–2002–1034, January 2002.
7. Hughes, C.E., "Aerodynamic Performance of Scale-Model Turbofan Outlet Guide Vanes Designed for Low Noise, " AIAA–2002–0374, January 2002.
8. Hughes, C.E., Jeracki, R.J., and Miller, C.J., "Fan Noise Source Diagnostic Test—Rotor Alone Aerodynamic Performance Results," AIAA–2002–2426, June 2002.
9. Podboy, G.G., Krupar, M.J., Helland, S.M., and Hughes, C.E., "Steady and Unsteady Flow Field Measurements Within a NASA 22 Inch Fan Model," AIAA–2002–1033, January 2002
10. Podboy, G.G., Krupar, M.J., Hughes, C.E., and Woodward, R.P., "Fan Source Diagnostic Test—LDV Measured Flow Field Results," AIAA–2002–2431, June 2002
11. Heidelberg, L.J., "Fan Noise Source Diagnostic Test—Tone Model Structure Results," AIAA–2002–2428, June 2002
12. Chestnutt, D., "Flight Effects of Fan Noise," NASA CP–2242, January 1982.

13. Balan, C., and Hoff, G.E., "Propulsion Simulator for High Bypass Turbofan Performance Evaluation," SAE Paper 931410, January 1993.
14. Ginder, R.B., and Newby, D.R., "An Improved Correlation for the Broadband Noise of High-Speed Fans," Journal of Aircraft, vol. 14, no. 9, September 1997, pp. 844–849.
15. Ganz, U., Joppa, P. Patten, T., and Scharpf, D., "Boeing 18-inch Fan Rig Broadband Noise Test," NASA/CR—1998-208704, 1998.
16. Joppa, P., "Experimental Investigation of Acoustic Characteristics of Broadband Noise Sources with the Boeing 18-inch Fan Rig, AIAA–99–1887, September, 1999.
17. Dahl, M.D., and Woodward, R.P., "Comparison Between Design and Installed Acoustic Characteristics of the NASA Lewis 9-by 15-Foot Low Speed Wind Tunnel Acoustic Treatment," NASA TP–2996, April 1990.
18. Dahl, M.D., and Woodward, R.P., "Background Noise Levels Measured I the NASA Lewis 9- by 15-Foot Low Speed Wind Tunnel," NASA TP–3274, November 1992.
19. Woodward, R.P., and Dittmar, J.H., "Background Noise Levels Measured in the NASA Lewis 9- by 15-Foot Low-Speed Wind Tunnel," NASA TM–106817, AIAA–95–0720, January 1995.

TABLE I – SOURCE DIAGNOSTIC TEST DESIGN PARAMETERS

Rotor

Rotor	No. Blades	L.E. Sweep	Design Tip Speed m/s (ft./s)	Design Stage Pressure Ratio
R4	22	0º	370 (1215)	1.47
M5	22	0º	411 (1350)	1.50

R4 was tested with three tip clearances: 0.004, 0.020, and 0.030 in.
Rotor-alone tests were with R4 and 0.020 in. tip clearance

Stator

Stator	No. Vanes	L.E. Sweep	Aspect Ratio	Solidity
Radial Baseline	54	0º	3.51	1.52
Radial Low-Count	26	0º	1.67	1.51
Swept	26	30º	1.67	1.53

Figure 1. Photograph of research fan installed in the NASA Glenn 9x15 LSWT.

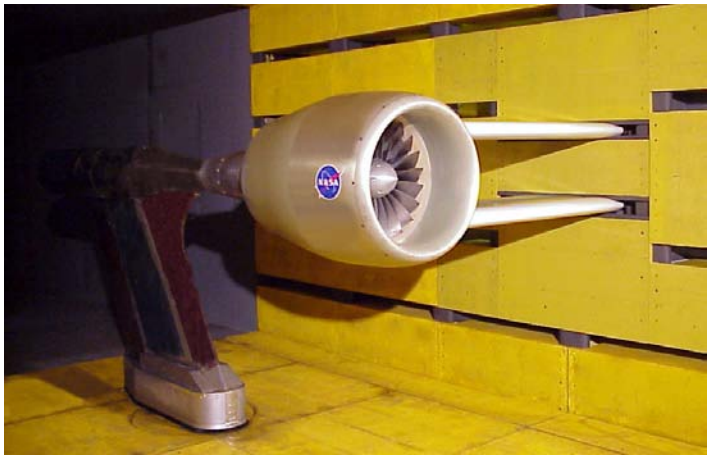

Figure 2. Photograph of Rotor-alone Nacelle (RAN) configuration in the NASA Glenn 9x15 LSWT.

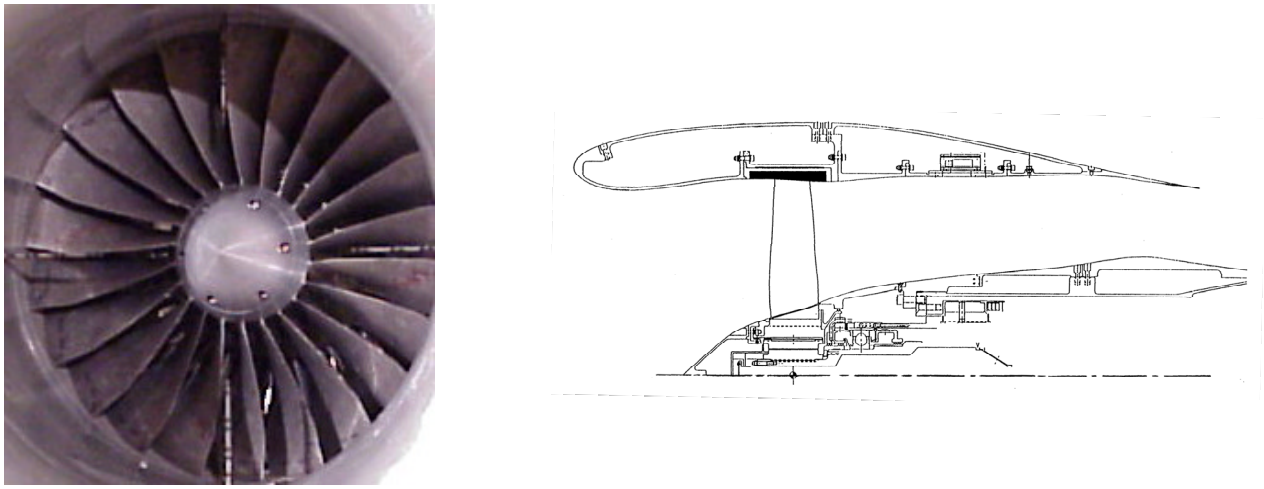

Figure 3. Photograph of the R4 rotor and sketch of the rotor-alone nacelle (RAN) configuration.

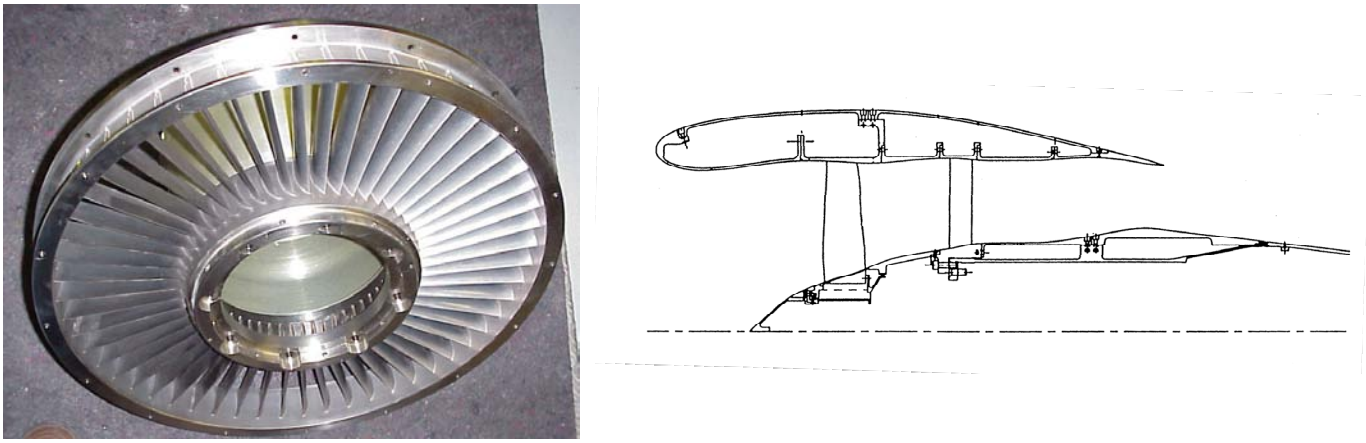

Figure 4. Photograph of the baseline 54-vane radial stator along with a sketch of the fan stage with the R4 rotor and this stator.

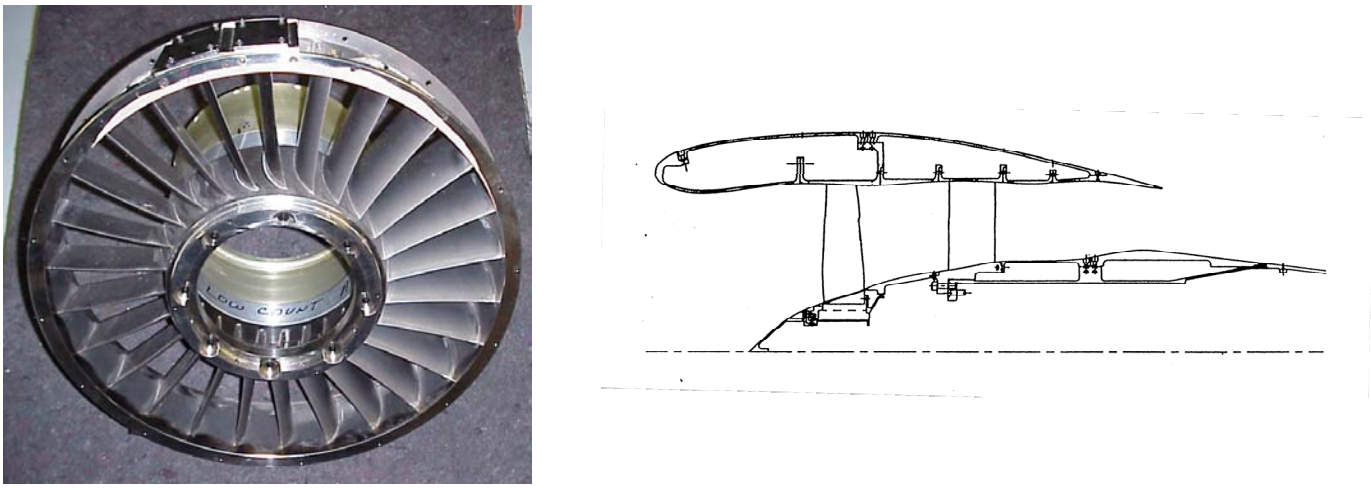

Figure 5. Photograph of the 26-vane "low-count" radial stator along with a sketch of the fan stage with the R4 rotor and this stator.

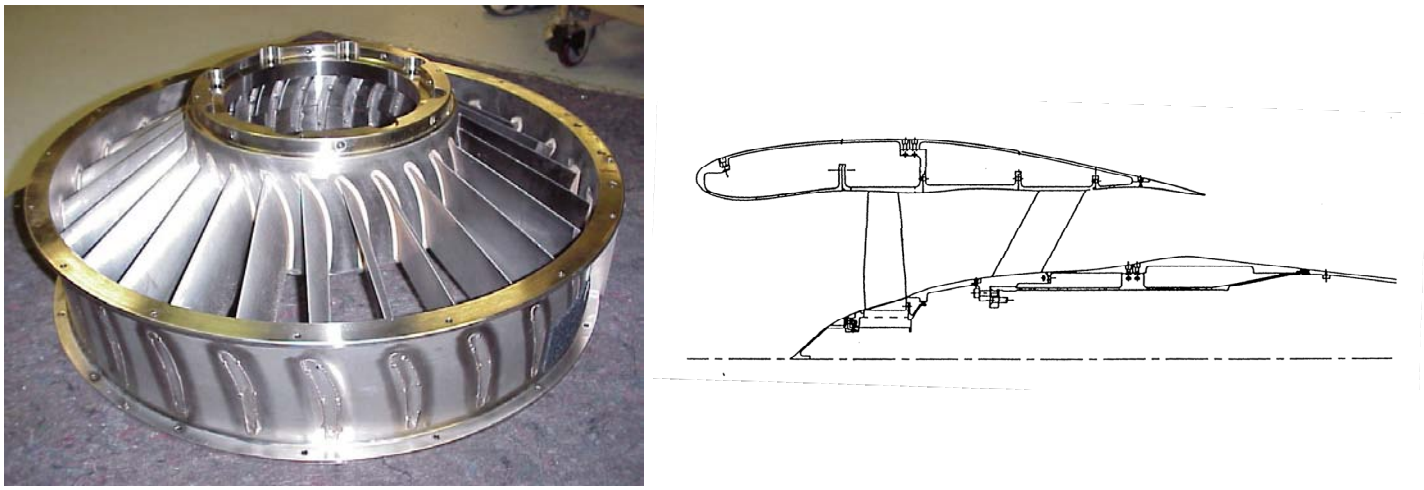

Figure 6. Photograph of the 26-vane "low-noise" swept stator along with a sketch of the fan stage with the R4 rotor and this stator.

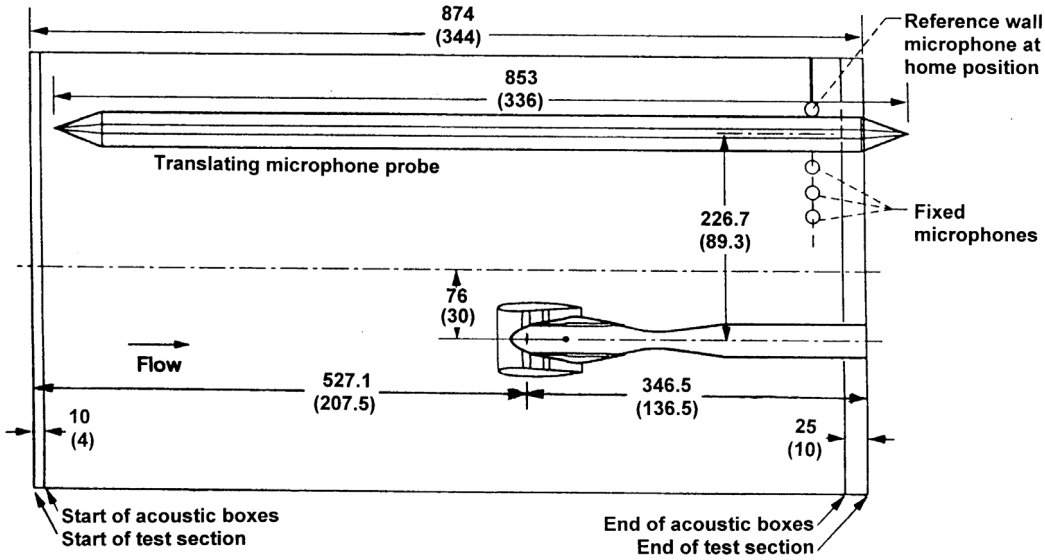

Figure 7. Sketch of the model fan installed in the 9- by 15-Foot Low Speed Wind Tunnel. Far-field acoustic data were acquired with a translating microphone probe and aft fixed microphones. (Dimensions in cm (in.)).

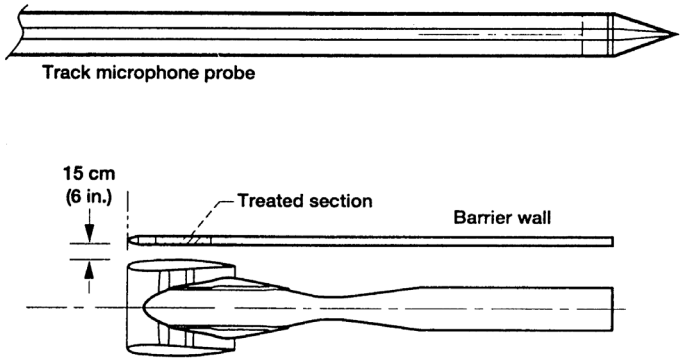

Figure 8. Sketch showing location of acoustic barrier wall relative to model fan. (Dimensions In cm (in)).

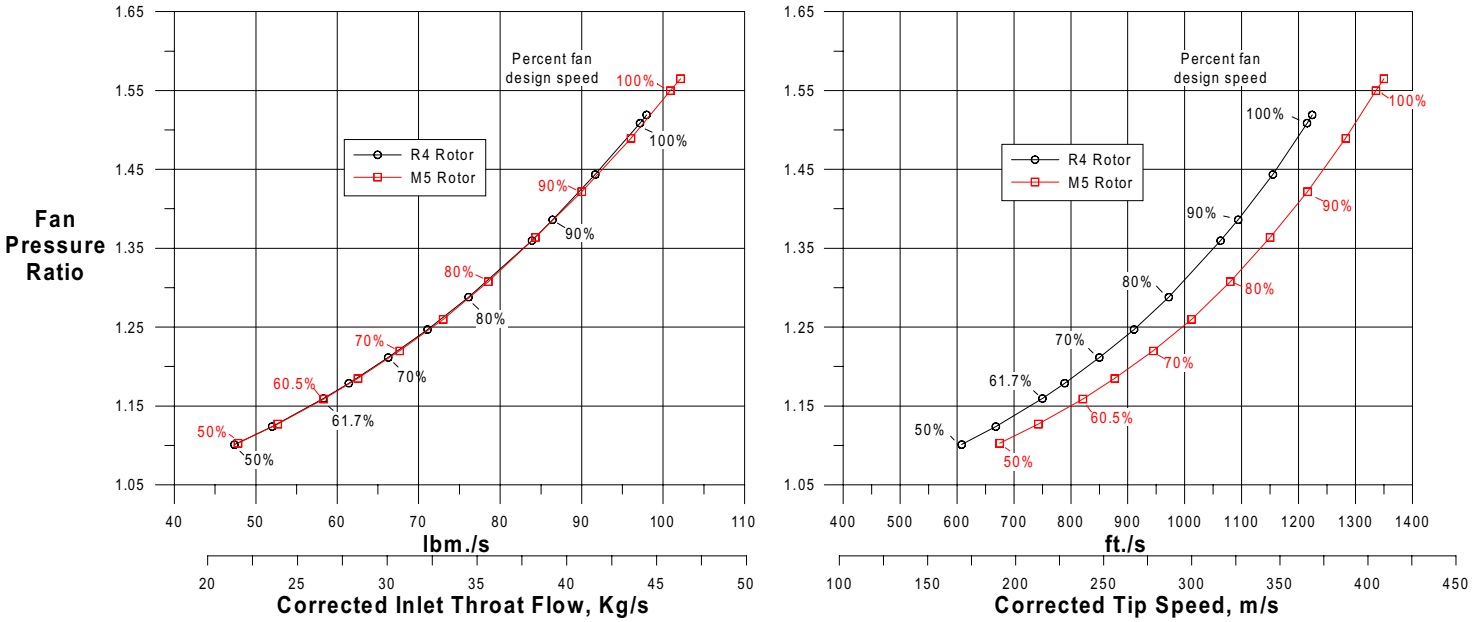

(a) Fan pressure ratio vs. corrected weight flow (b) Fan pressure ratio vs. corrected tip speed

Figure 9. Aero performance for the R4 and M5 rotors with the baseline radial stator.

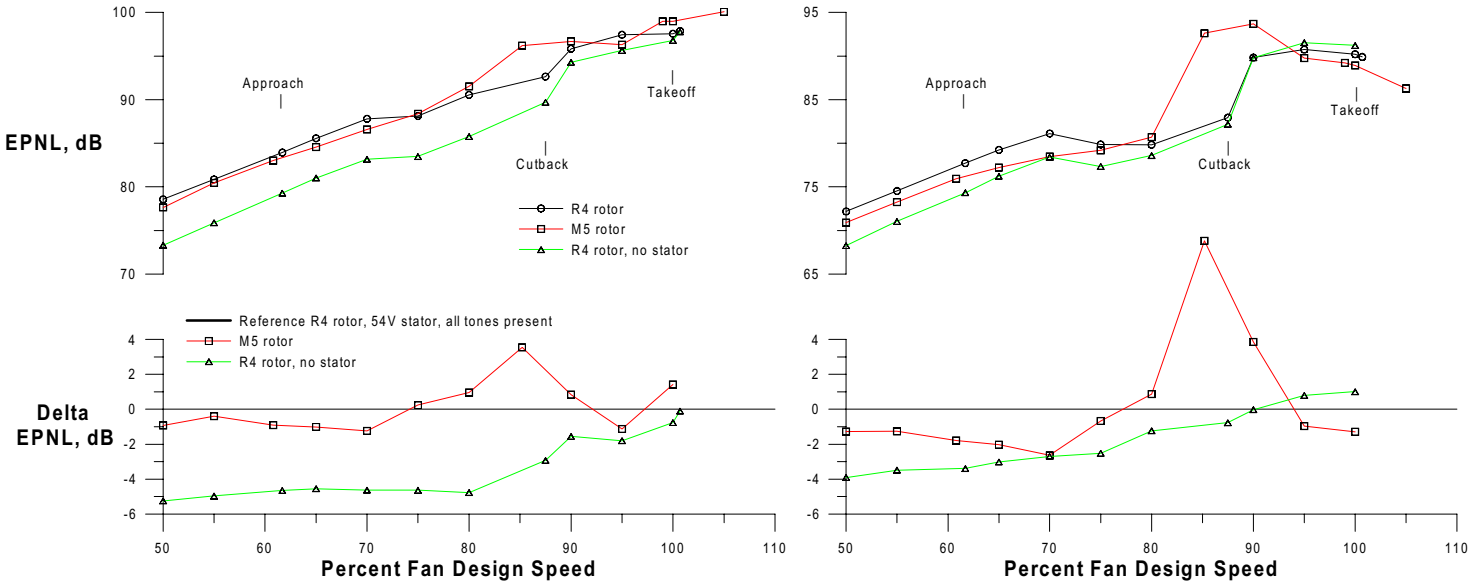

(a) No Barrier Wall (b) Barrier wall in place

Figure 10. EPNL for 54-vane baseline stator with all tones present.

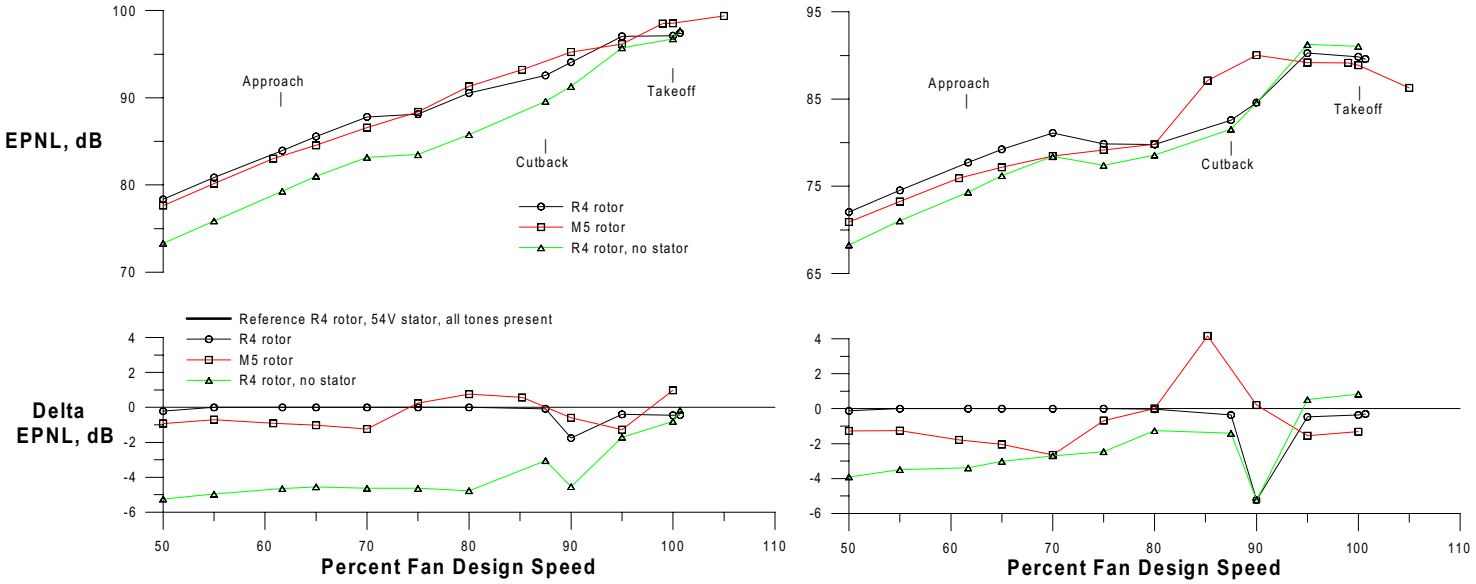

(a) No Barrier Wall (b) Barrier wall in place

Figure 11. EPNL for 54-vane baseline stator with BPF tone removed.

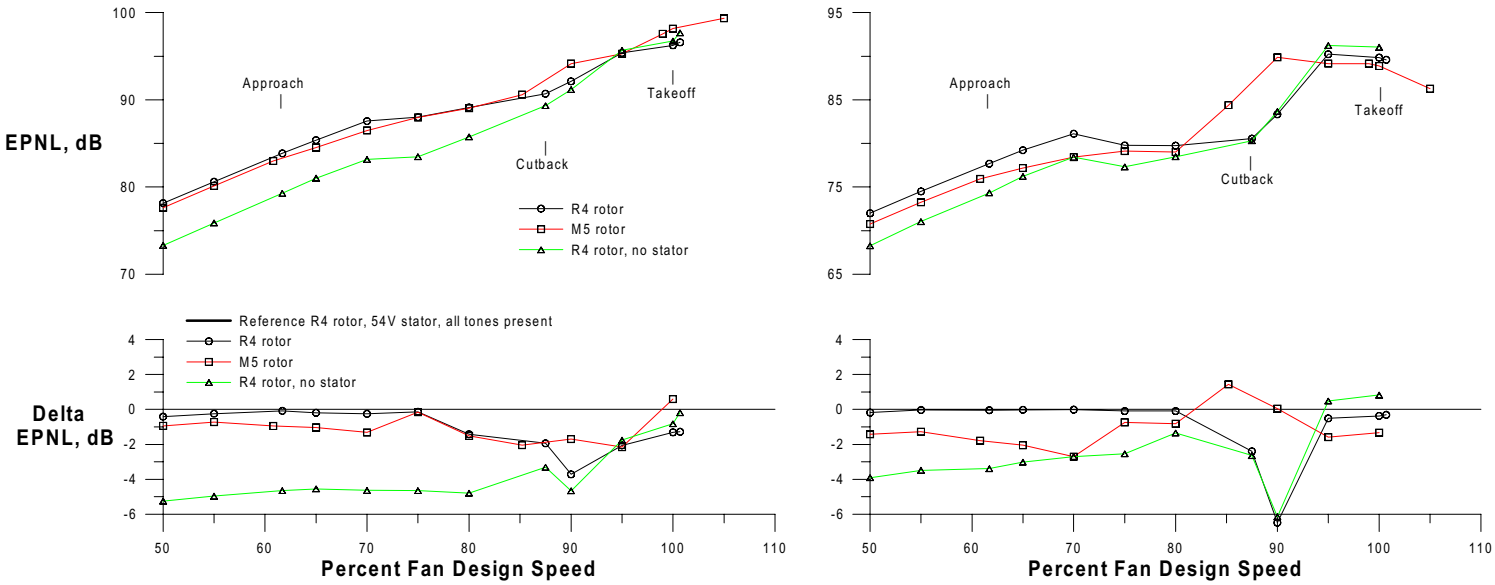

(a) No Barrier Wall (b) Barrier wall in place

Figure 12. EPNL for 54-vane baseline stator with all tones (except MPTs) removed.

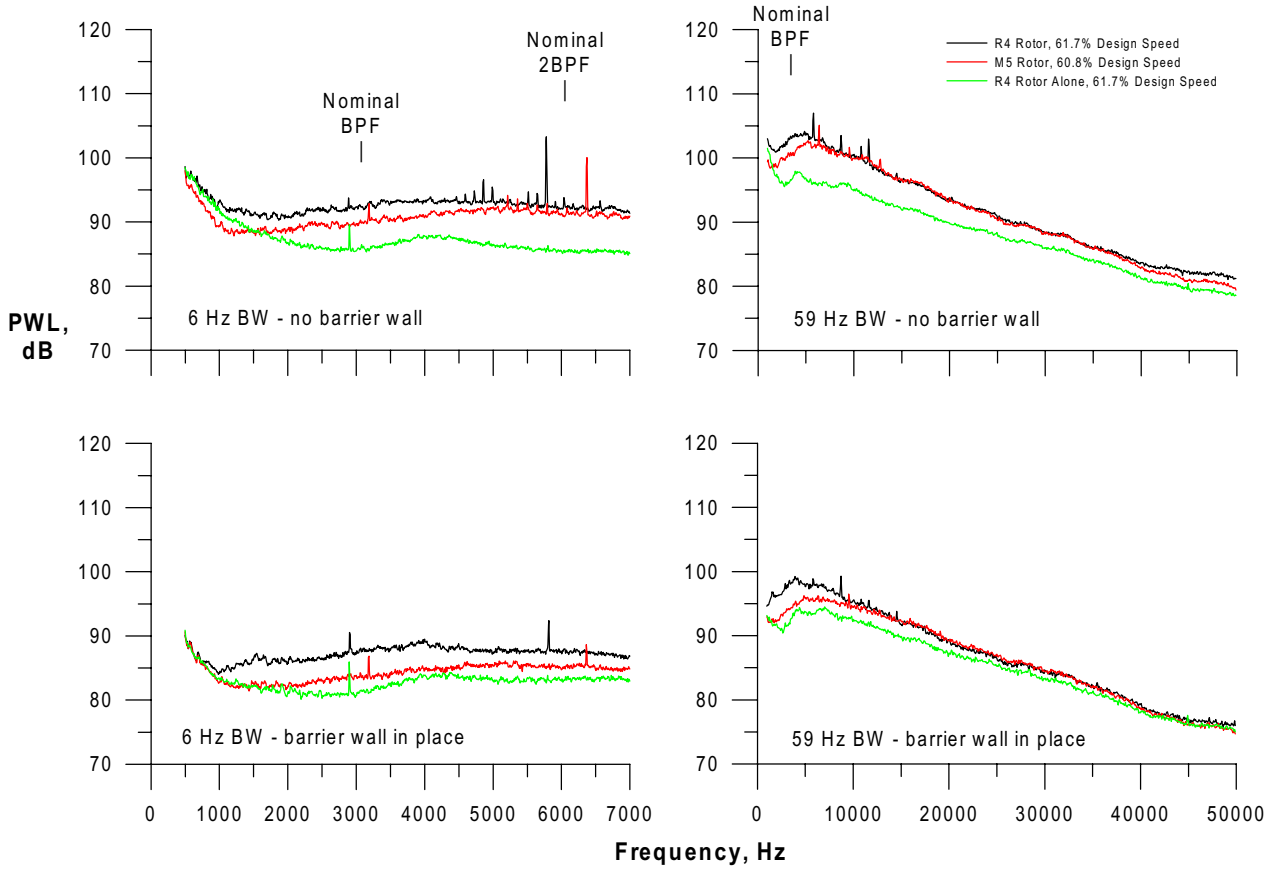

Figure 13. PWL spectra for 54-vane baseline stator at nominal 61% design fan speed.

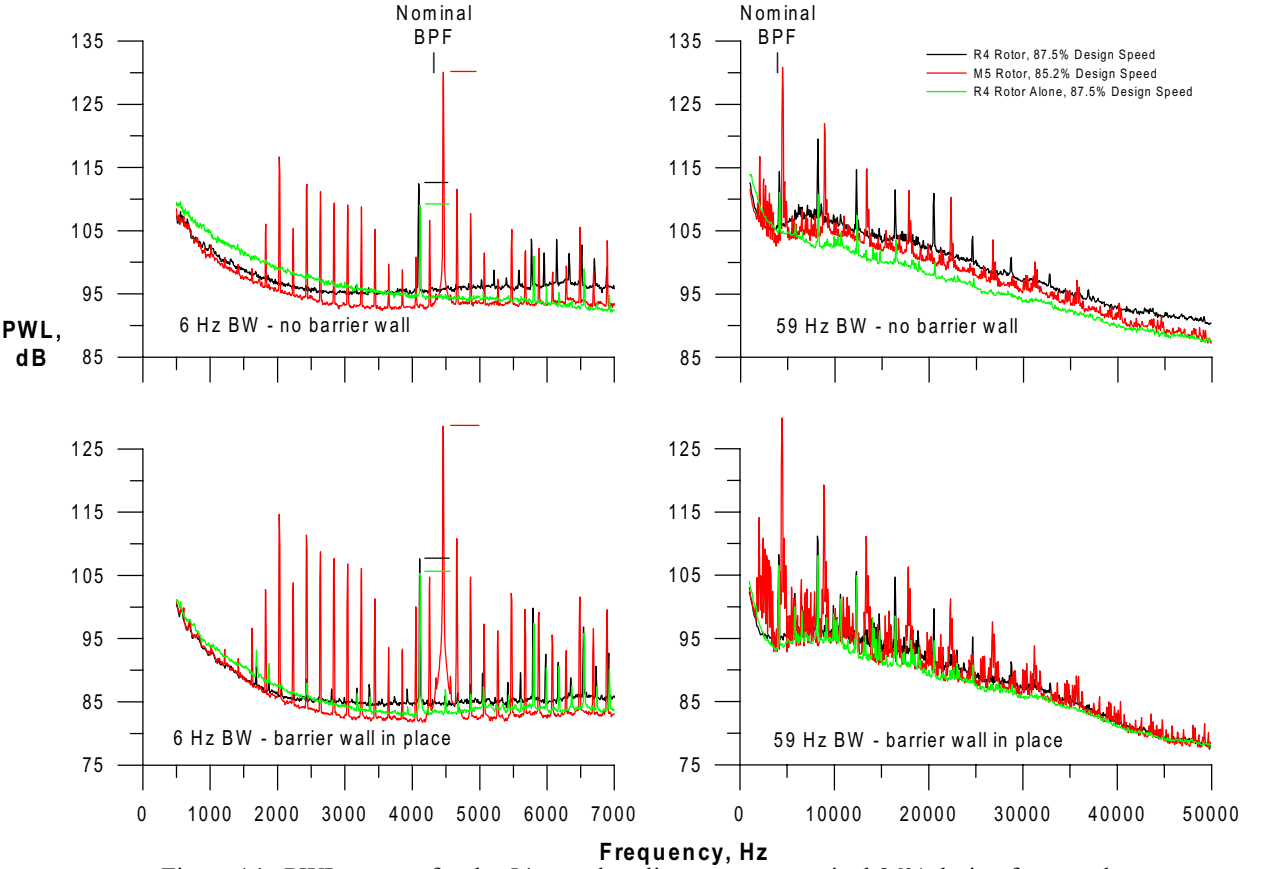

Figure 14. PWL spectra for the 54-vane baseline stator at nominal 86% design fan speed.

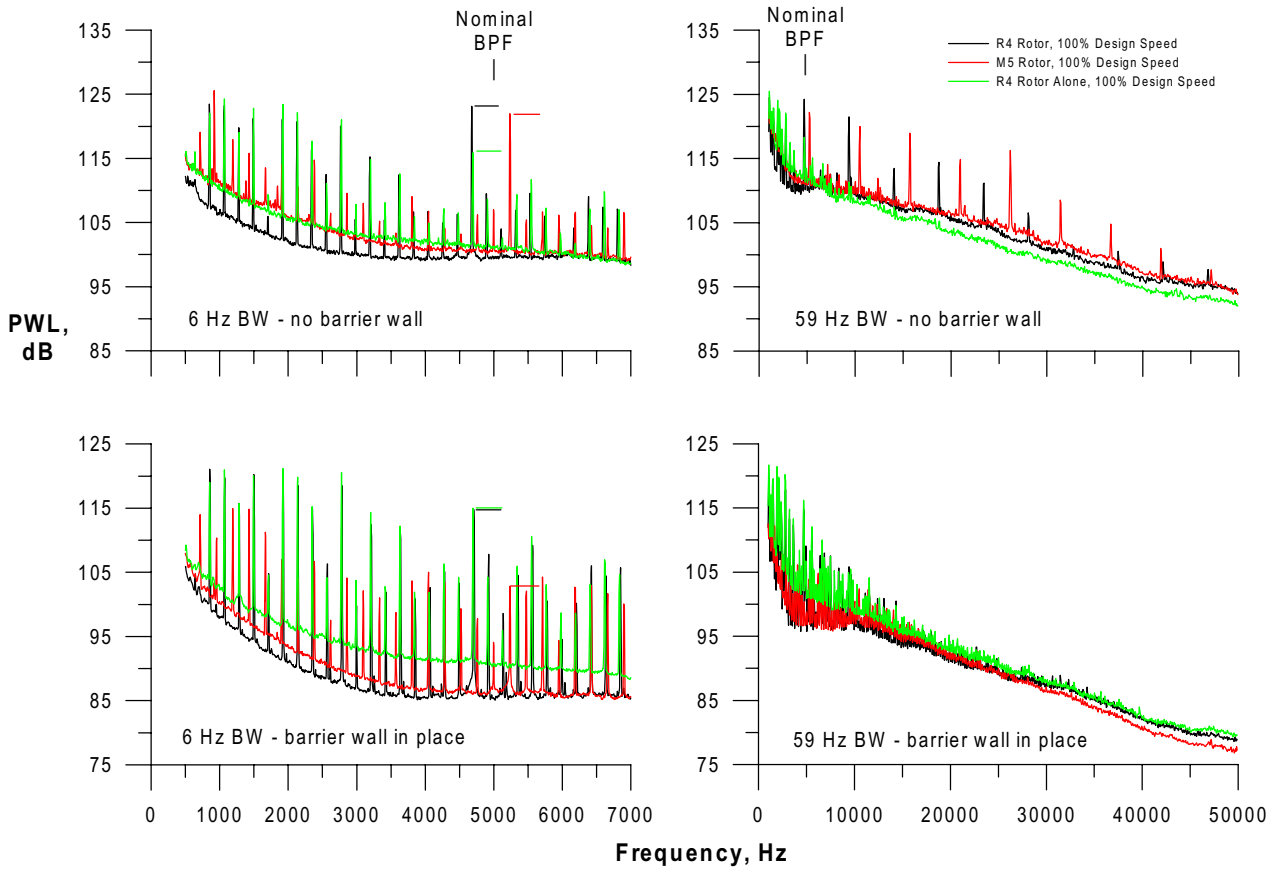

Figure 15. PWL spectra for the 54-vane baseline stator at 100% design fan speed.

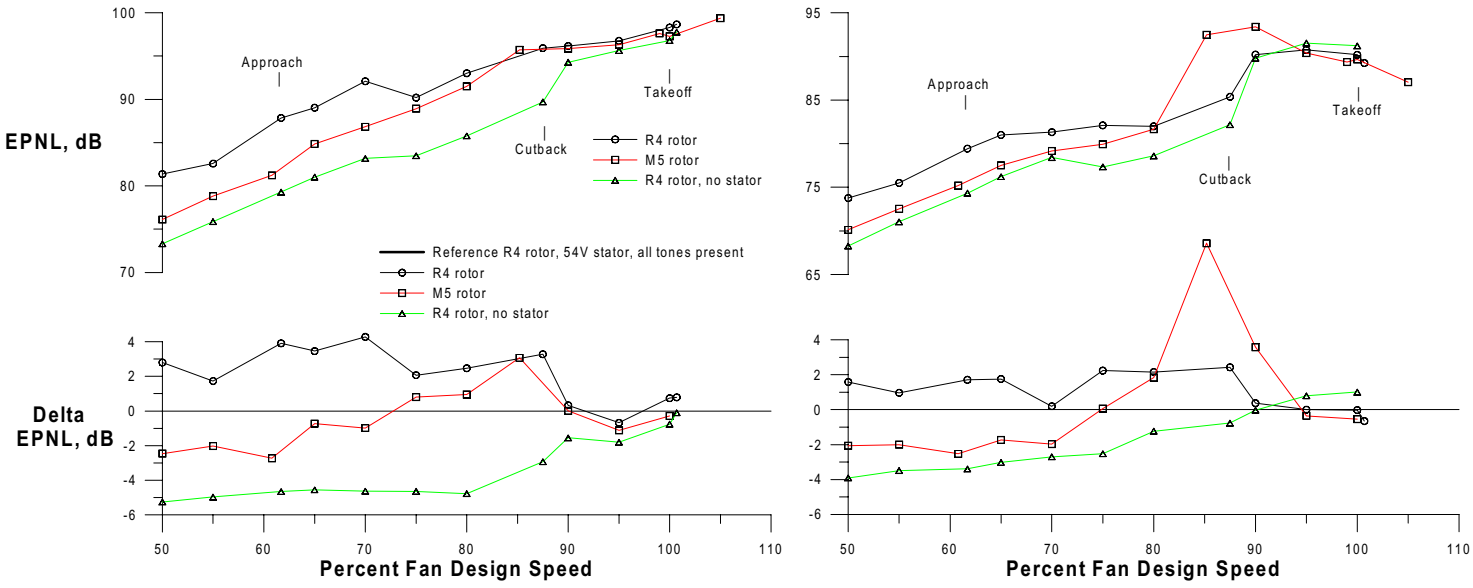

(a) No Barrier Wall

(b) Barrier wall in place

Figure 16. EPNL for 26-vane radial stator with all tones present.

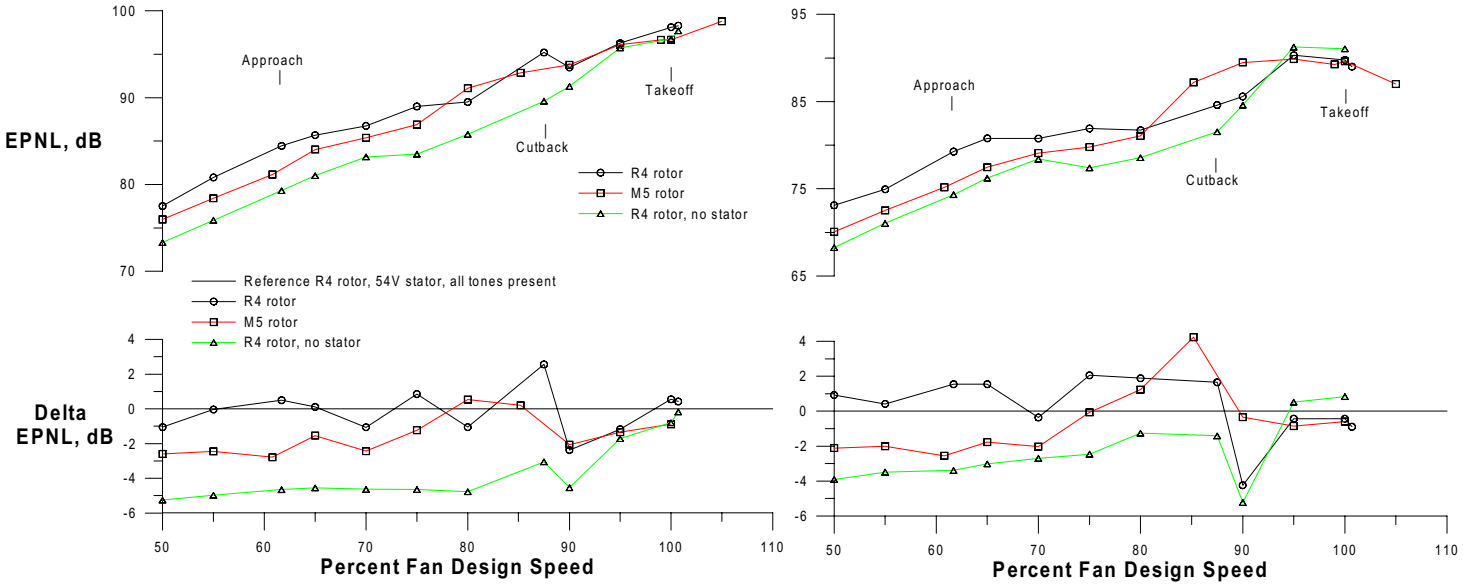

(a) No Barrier Wall (b) Barrier wall in place

Figure 17. EPNL for 26-vane radial stator with BPF tone removed.

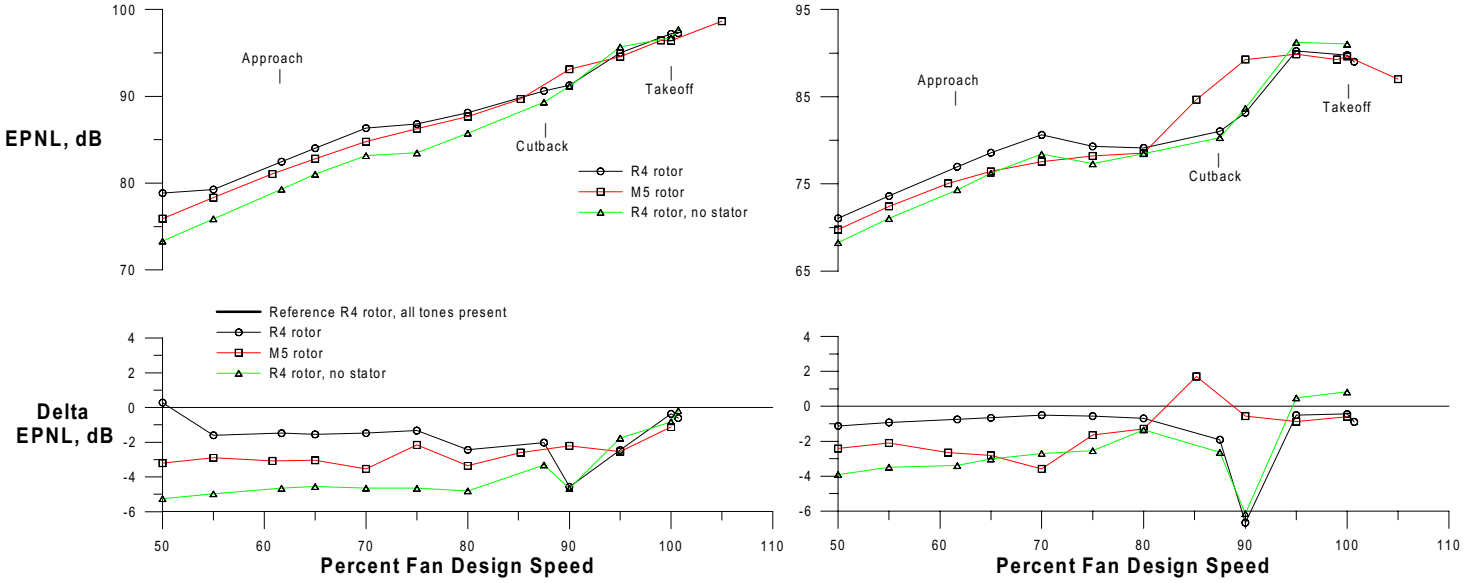

(a) No Barrier Wall (b) Barrier wall in place

Figure 18. EPNL for 26-vane radial stator with all tones (except MPTs) removed.

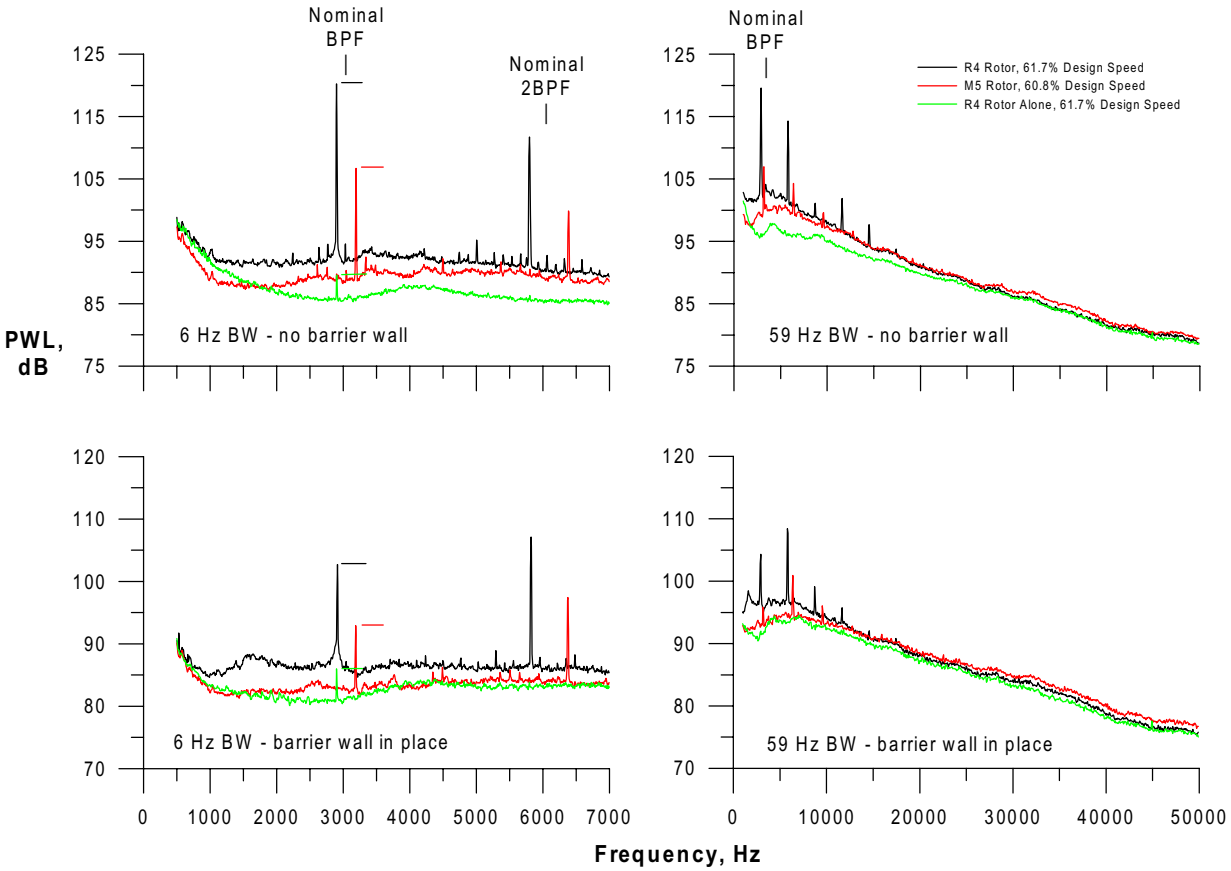

Figure 19. PWL spectra for the 26-vane radial stator at nominal 61% design fan speed.

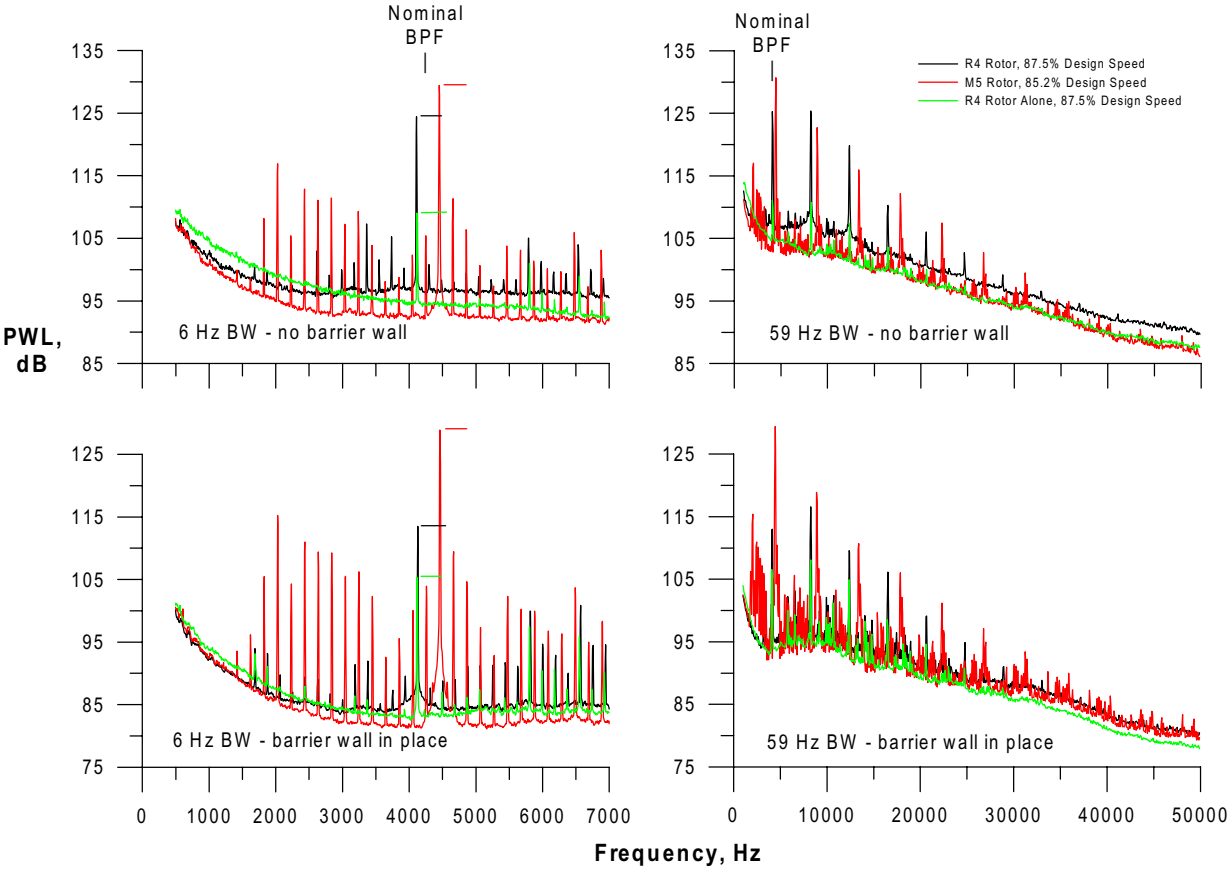

Figure 20. PWL spectra for the 26-vane radial stator at nominal 86% design fan speed.

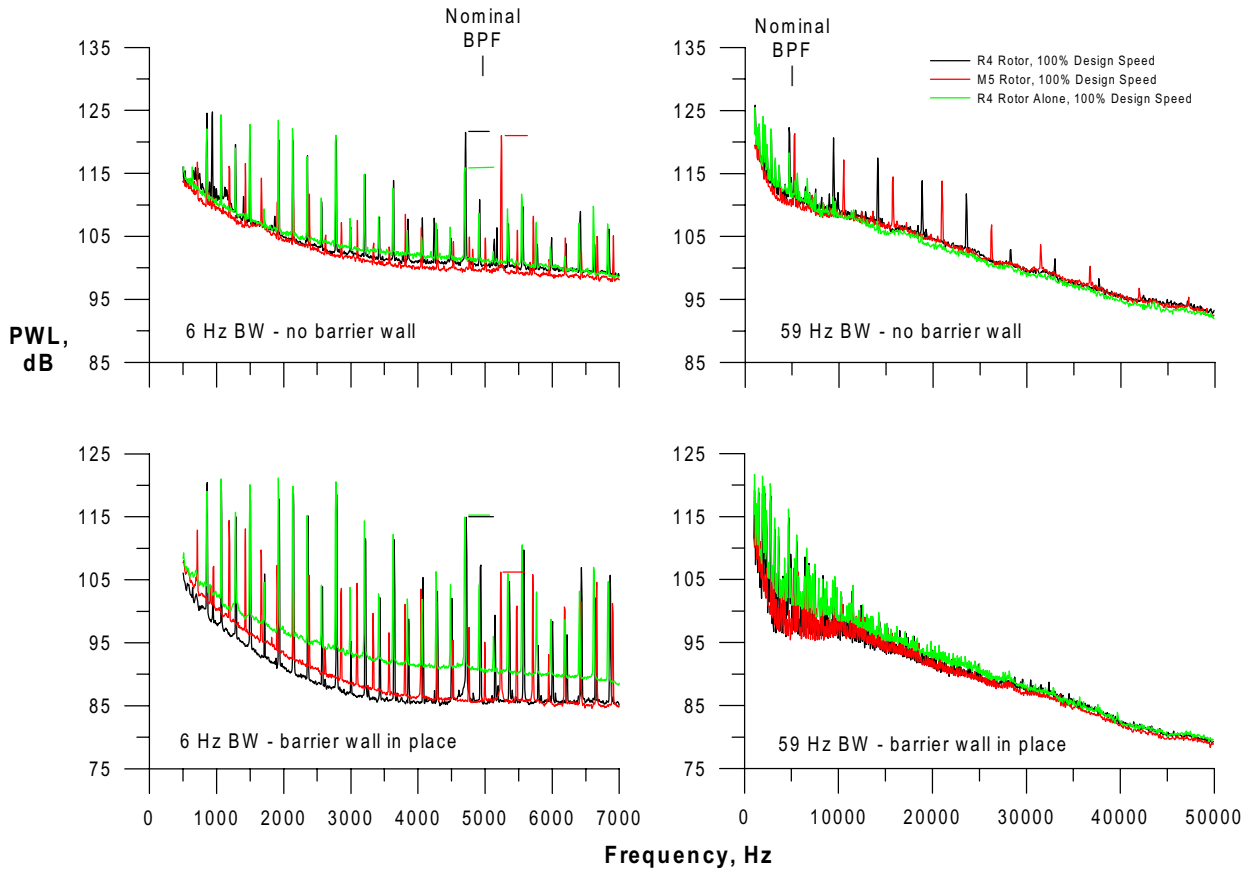

Figure 21. PWL spectra for the 26-vane radial stator at 100% design fan speed.

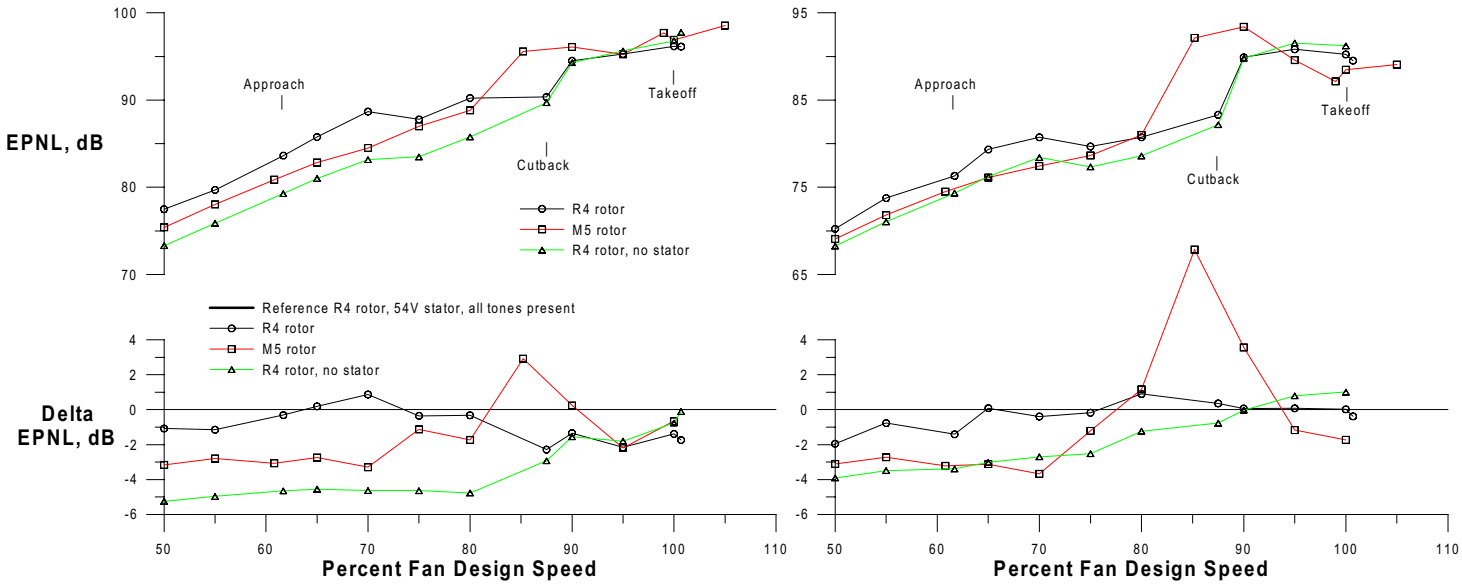

(a) No Barrier Wall

(b) Barrier wall in place

Figure 22. EPNL for 26-vane swept stator with all tones present.

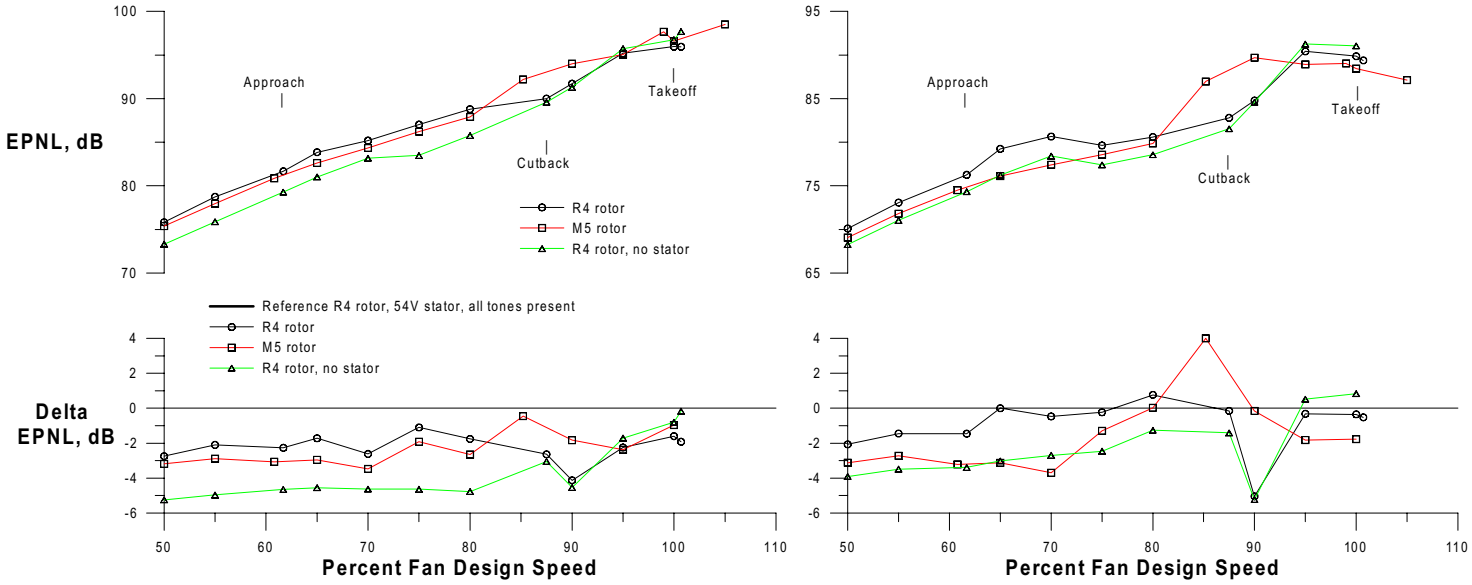

(a) No Barrier Wall (b) Barrier wall in place

Figure 23. EPNL for 26-vane swept stator with BPF tone removed.

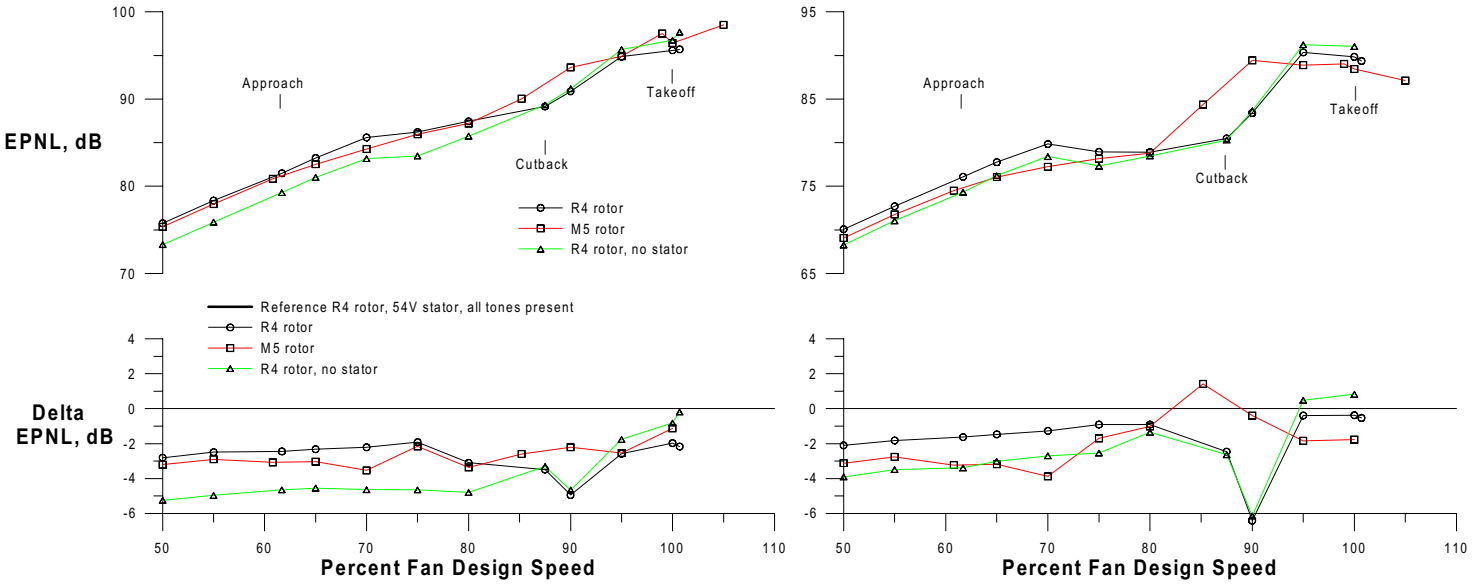

(a) No Barrier Wall (b) Barrier wall in place

Figure 24. EPNL for 26-vane swept stator with all tones (except MPTs) removed.

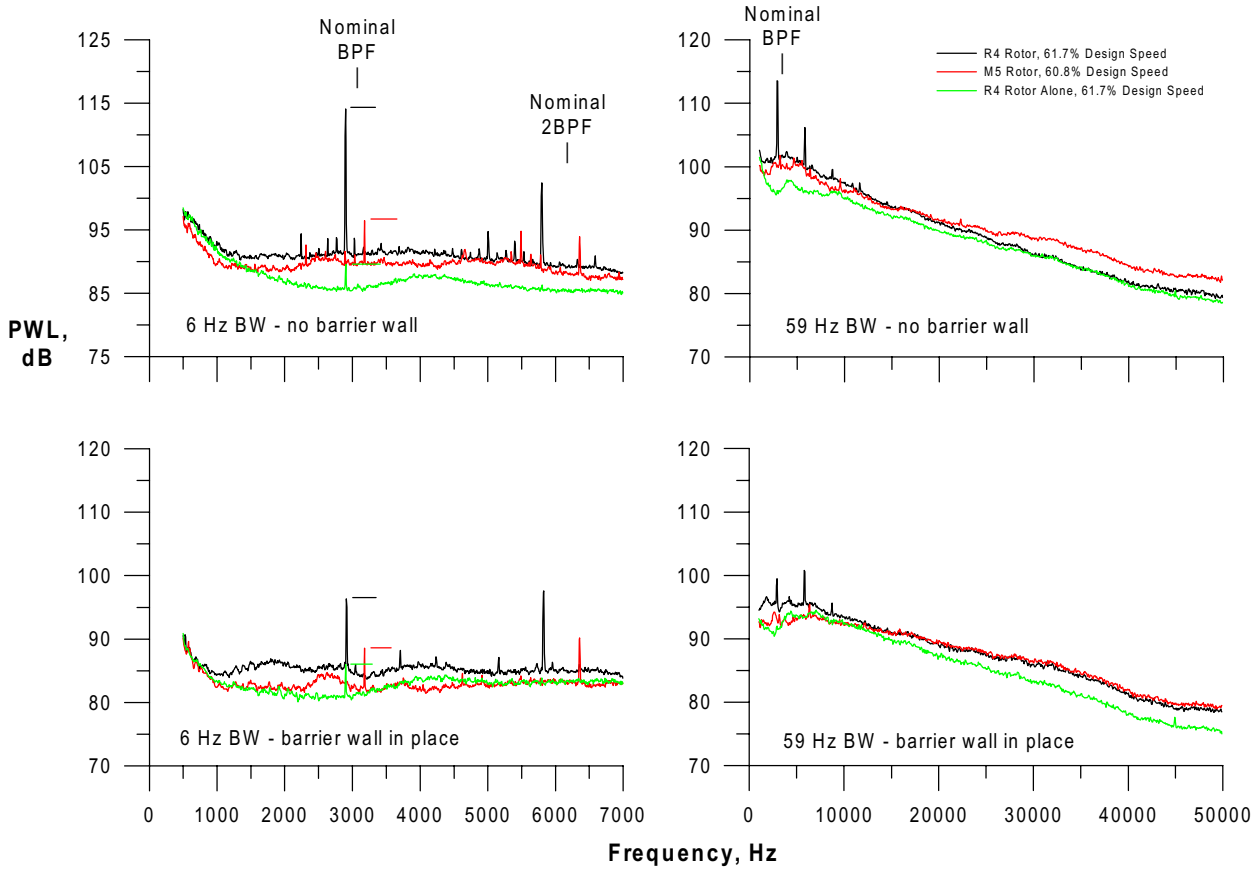

Figure 25. PWL spectra for the 26-vane swept stator at nominal 61% design fan speed.

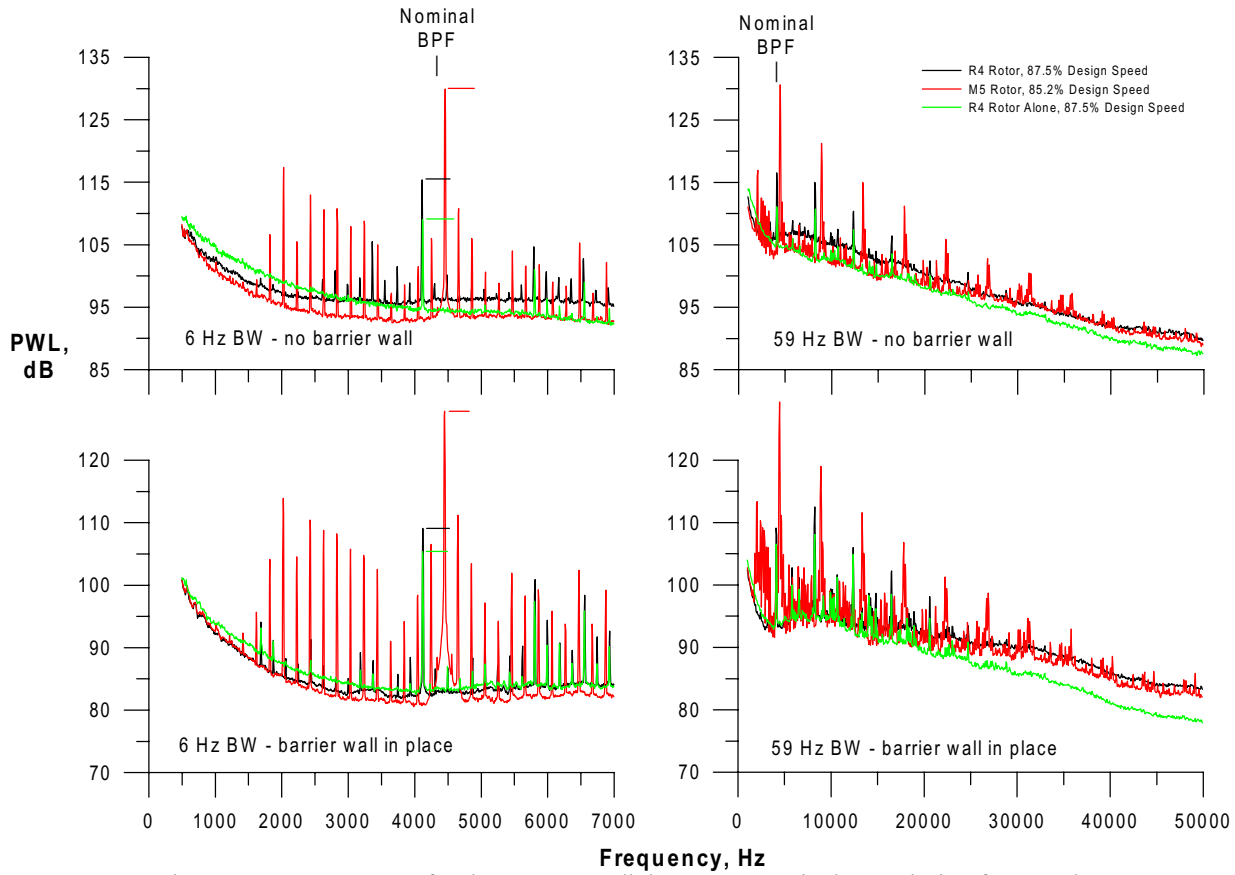

Figure 26. PWL spectra for the 26-vane radial stator at nominal 86% design fan speed.

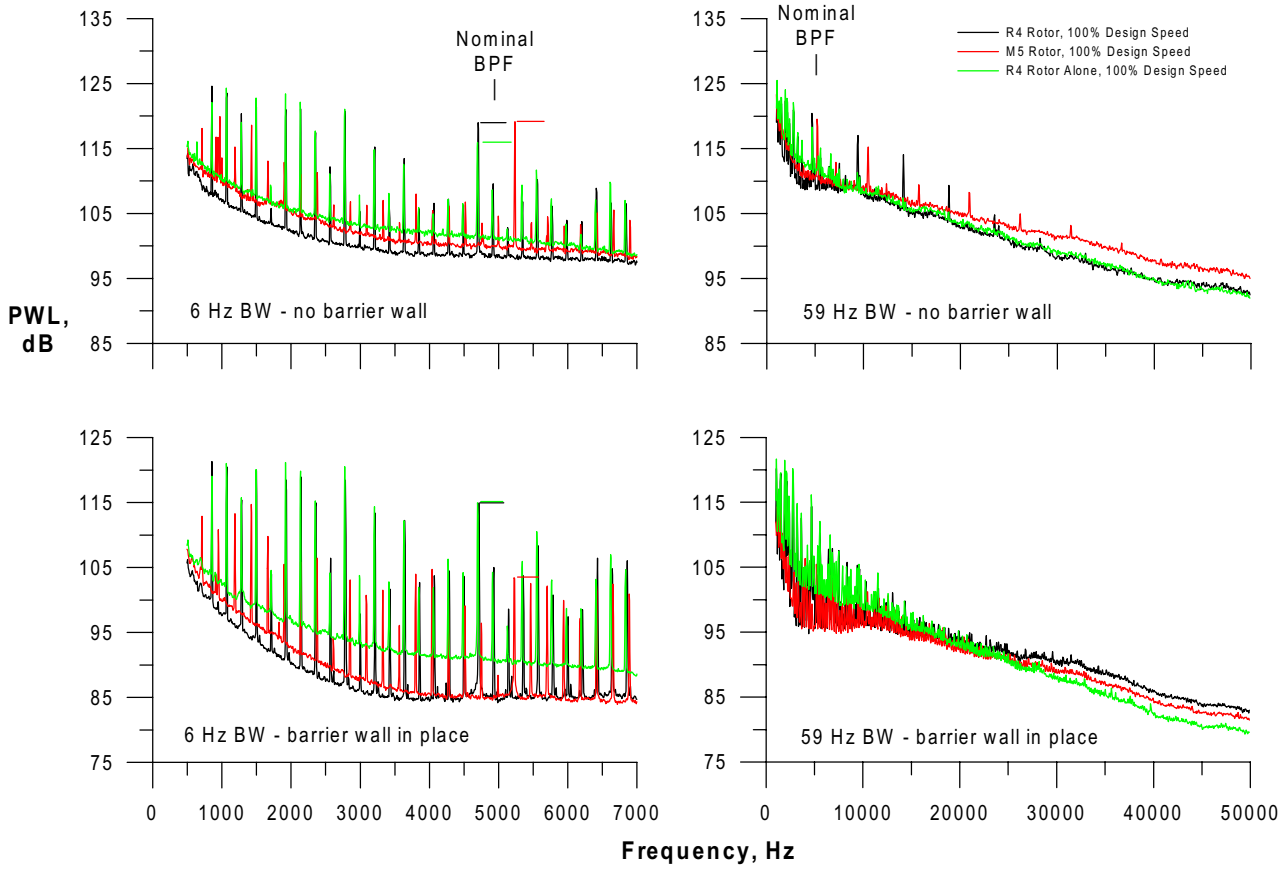

Figure 27. PWL spectra for the 26-vane swept stator at 100% design fan speed.

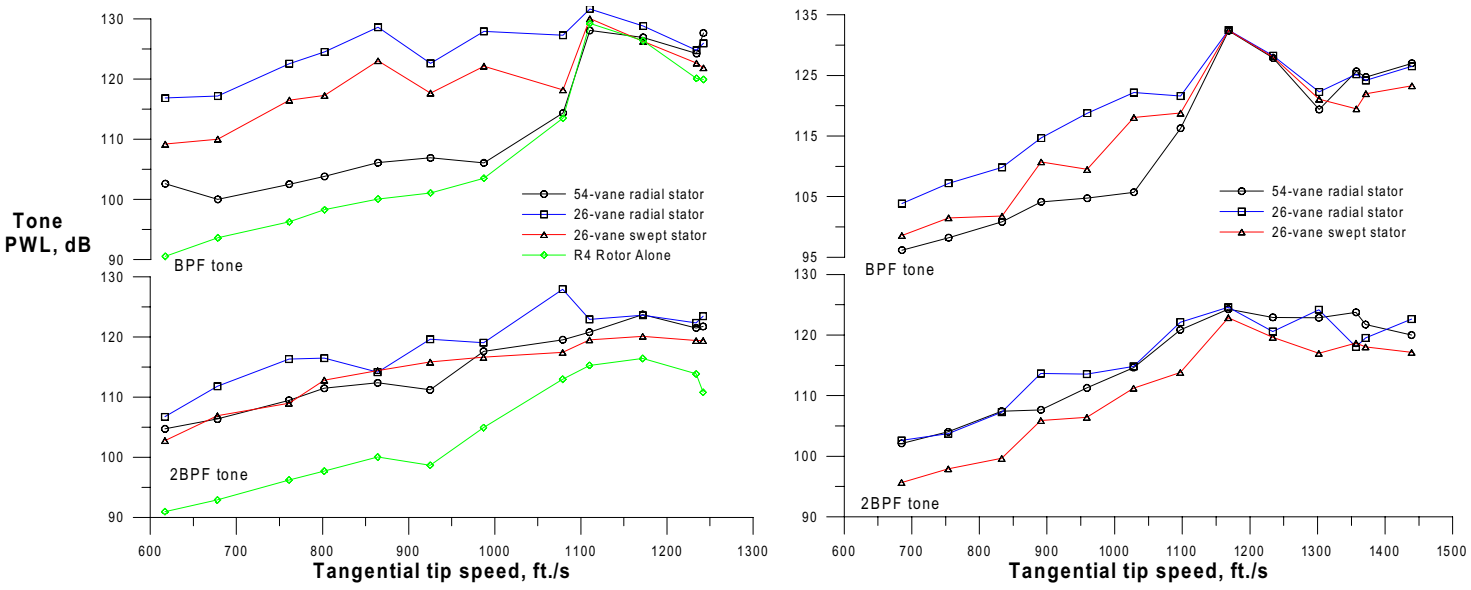

(a) R4 rotor

(b) M5 rotor

Figure 28. PWL tone levels for the three stator sets (R4 .020 in. tip clearance, M5 nominal tip clearance).

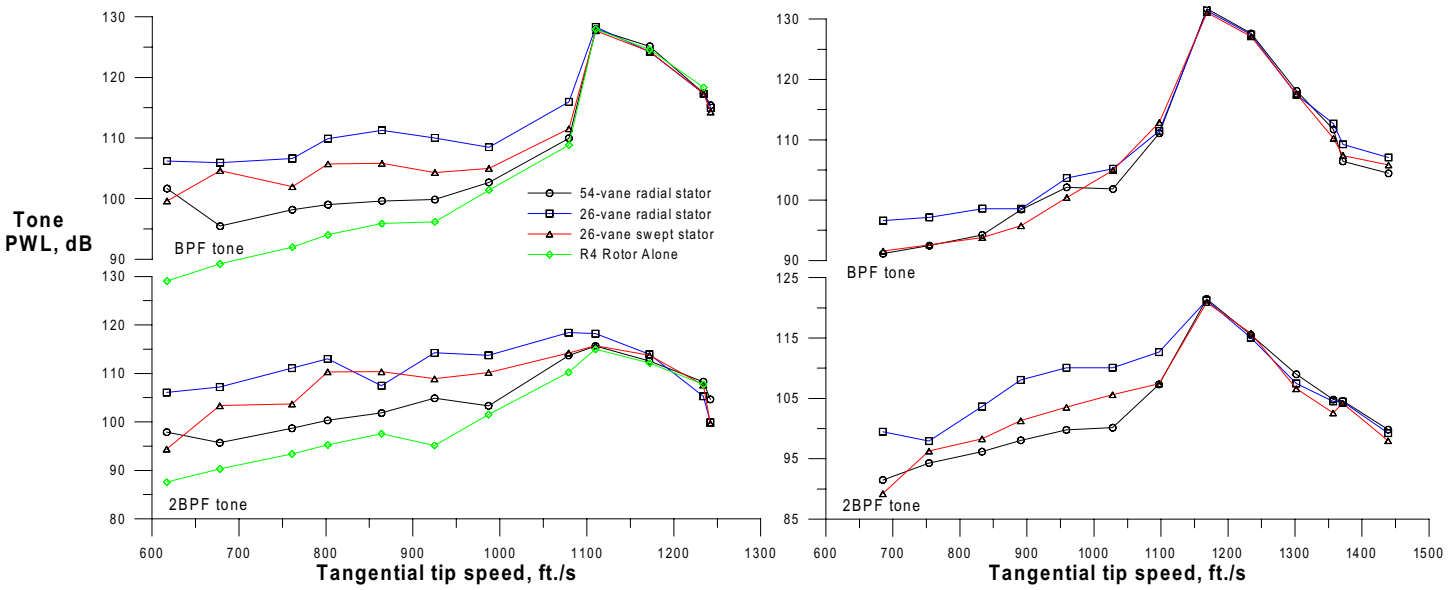

(a) R4 rotor (b) M5 rotor

Figure 29. PWL tone levels for the three stator sets, acoustic barrier wall in place (R4 .020 in. tip clearance, M5 nominal tip clearance).

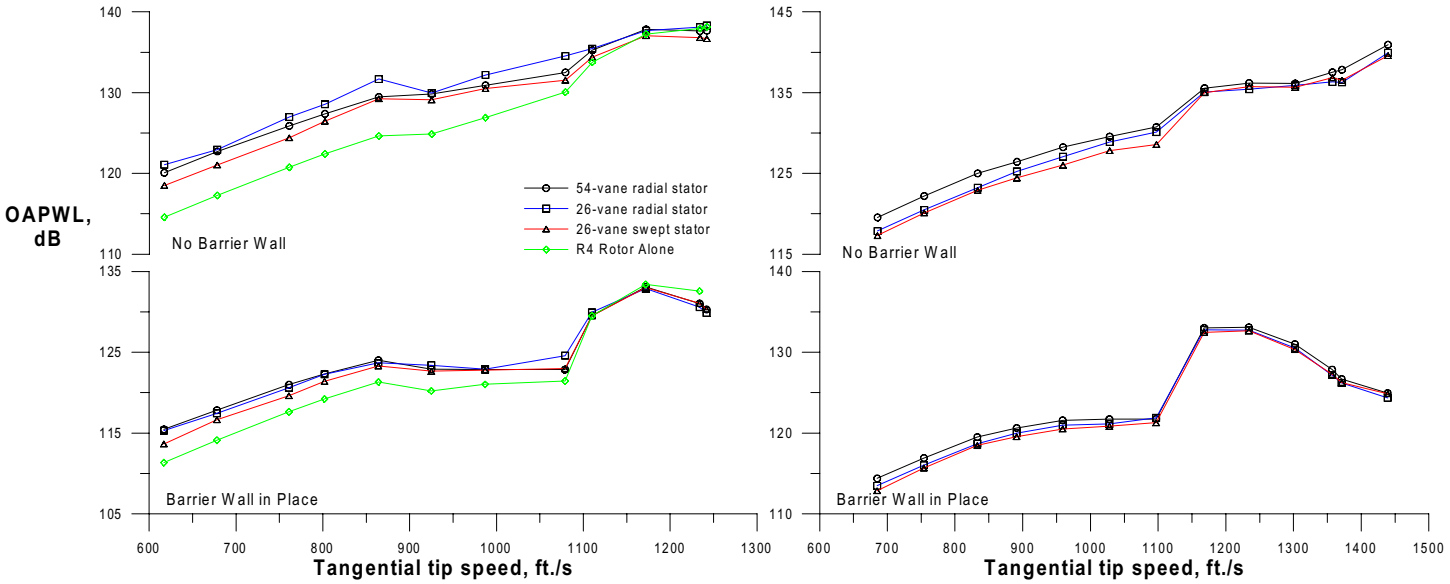

(a) R4 rotor (b) M5 rotor

Figure 30. OAPWL for the three stator sets (OAPWL integrated from 1K to 50K Hz, R4 .020 in. tip clearance, M5 nominal tip clearance).

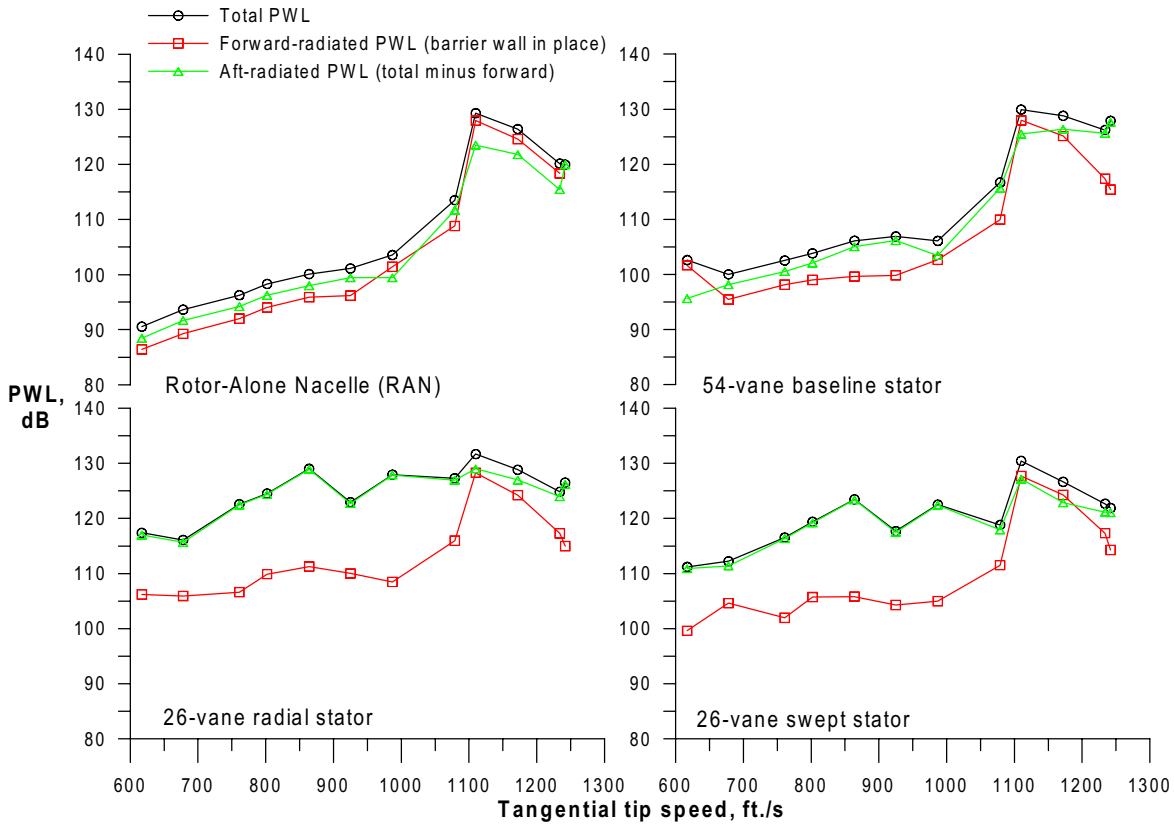

Figure 31. Total sideline, forward-radiating (wall), and aft-radiating (total minus wall) BPF tone sound power for the R4 rotor alone (RAN) and with three stator sets.

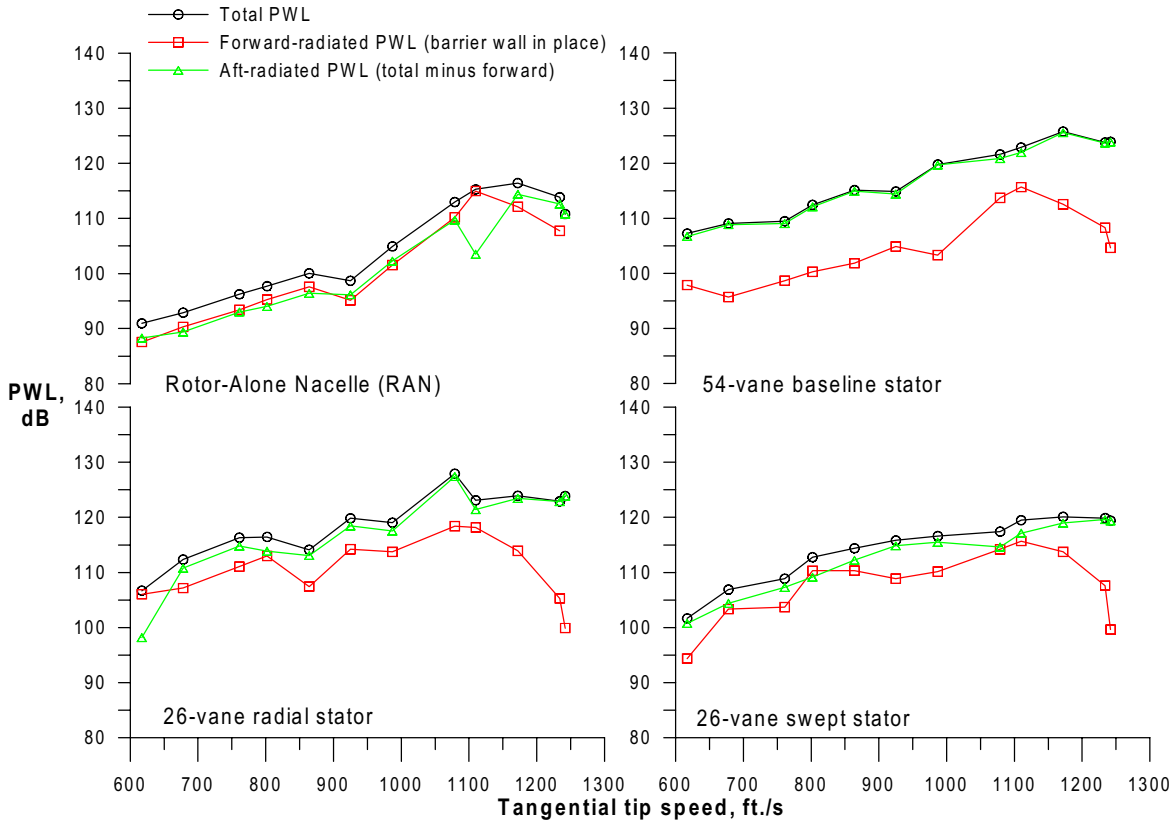

Figure 32. Total sideline, forward-radiating (wall), and aft-radiating (total minus wall) 2BPF tone sound power for the R4 rotor alone (RAN) and with three stator sets.

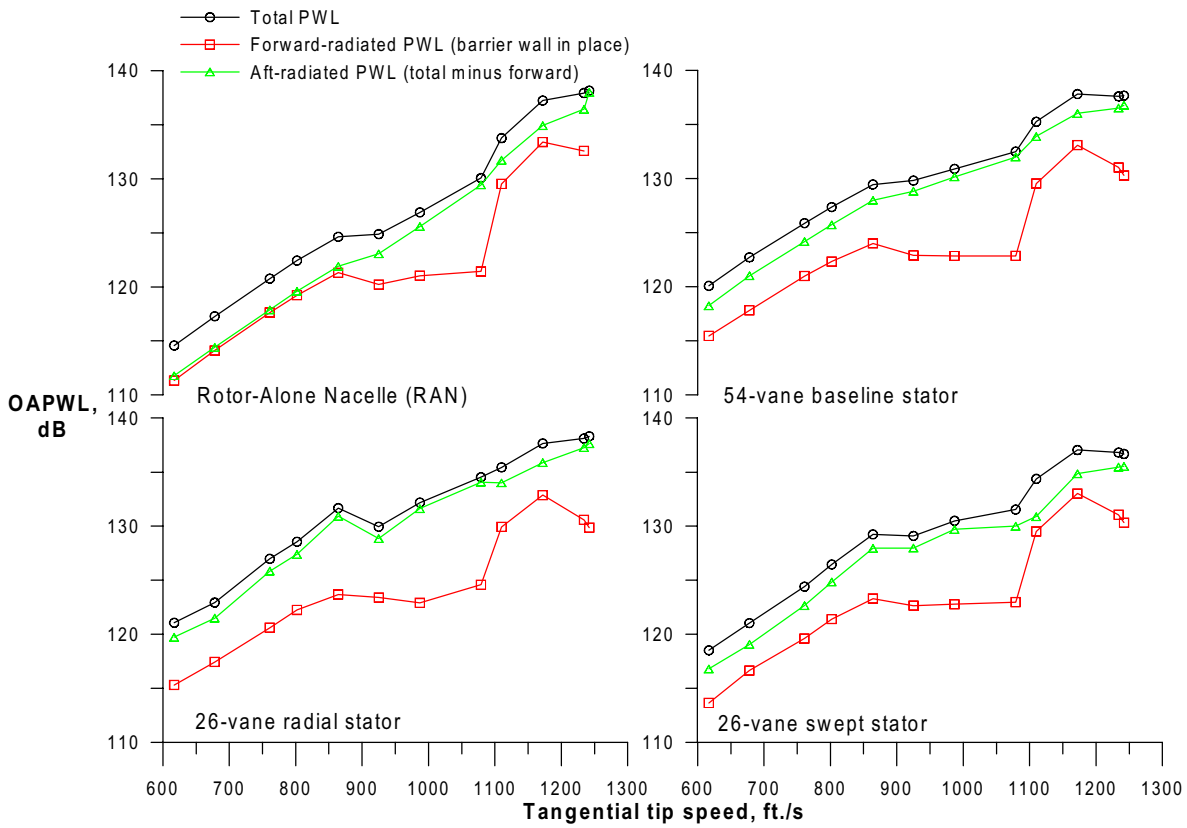

Figure 33. Total sideline, forward-radiating (wall), and aft-radiating (total minus wall) OAPWL for the R4 rotor alone (RAN) and with three stator sets.

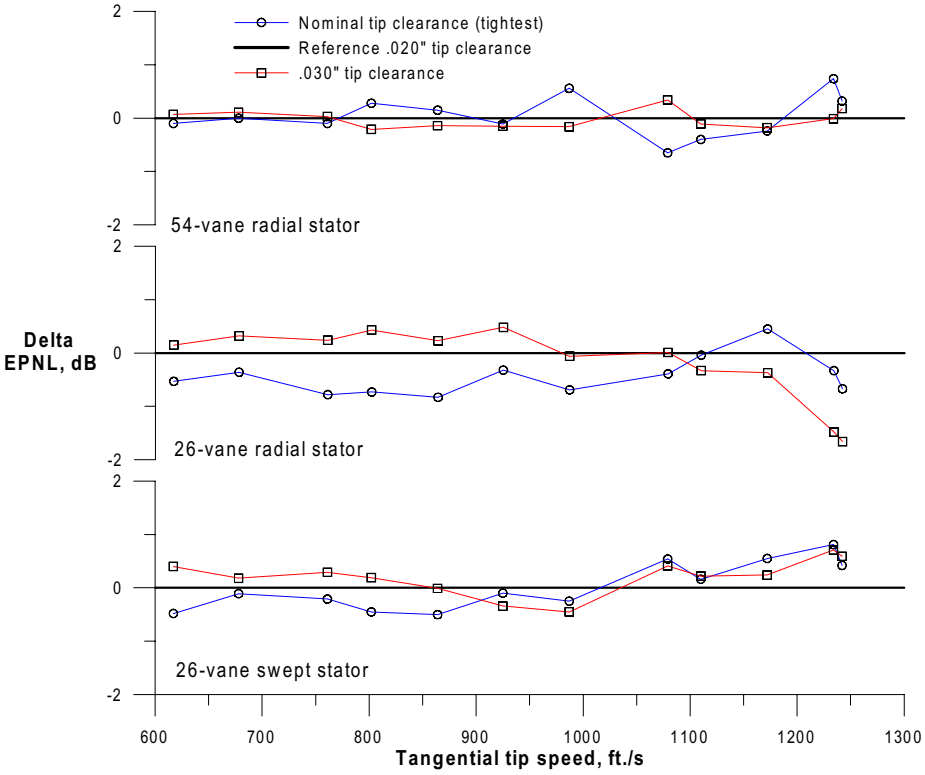

Figure 34. Effects of R4 rotor tip clearance on EPNL.

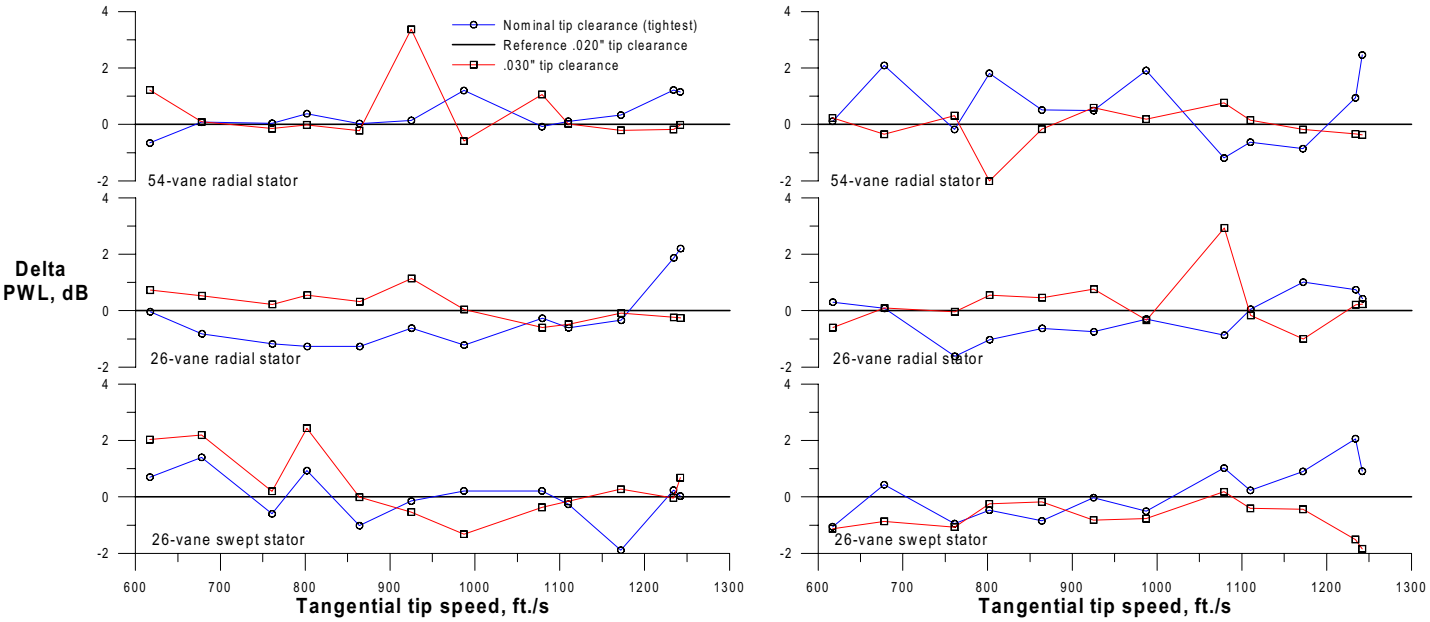

(a) BPF tone

(b) 2BPF tone

Figure 35. Effects of R4 rotor tip clearance on tone PWL.